



The Abdus Salam  
International Centre for Theoretical Physics

  
United Nations  
Educational, Scientific  
and Cultural Organization

  
International Atomic  
Energy Agency




**SMR.1661 - 2**

**Conference on**  
**VORTEX RINGS AND FILAMENTS IN CLASSICAL AND QUANTUM SYSTEMS**  
**6 - 8 June 2005**

**Dynamics of Vortex Rings in a Rotating Fluid**

**R. Verzicco**  
**Politecnico di Bari, Italy**

classical  
Dynamics of a  $\checkmark$  vortex ring  
in a rotating environment


R. Verzicco 

A.H.M. Eisenga \*

G.J.F. van Heijst \*

P. Orlandi †

G.F. Carnevale °

 DIMeG and CEMeC, Politecnico di Bari  
Italy

† Dipartimento di Meccanica e Aeronautica  
Università di Roma "La Sapienza" Italia

\* Fluid Dynamics Laboratory Eindhoven University of  
Technology, Eindhoven The Netherlands.

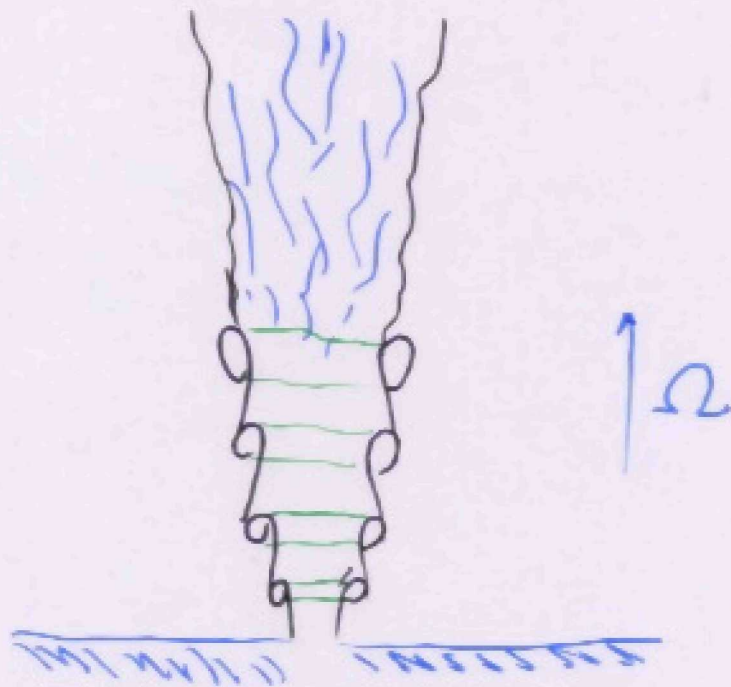
° Scripps Institution of Oceanography University of  
California, San Diego, La Jolla, USA.

## Motivation

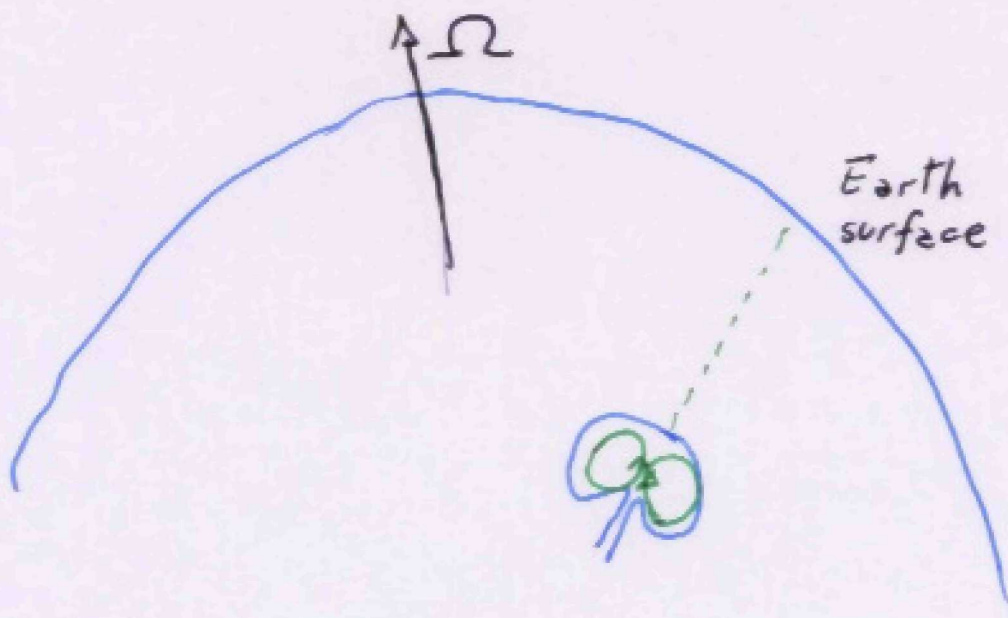
- Geophysical flows
- Flows in turbo-machineries  
(interaction between mean flow and imposed rotation)
- "Simple structure"  
complex vorticity dynamics
- One single structure  $\rightarrow$  detailed investigation

vortex ring  $\parallel$  to background rotation

vortex ring  $\perp$  to background rotation



The penetration of the plumes is reduced by the ambient rotation (Ayotte & Fernando 1986)



Slow upward motion of "mushroom-like" structures

Depending on the latitude the ambient rotation has different components  $\parallel$  and  $\perp$  to the motion

# Experimental set-up

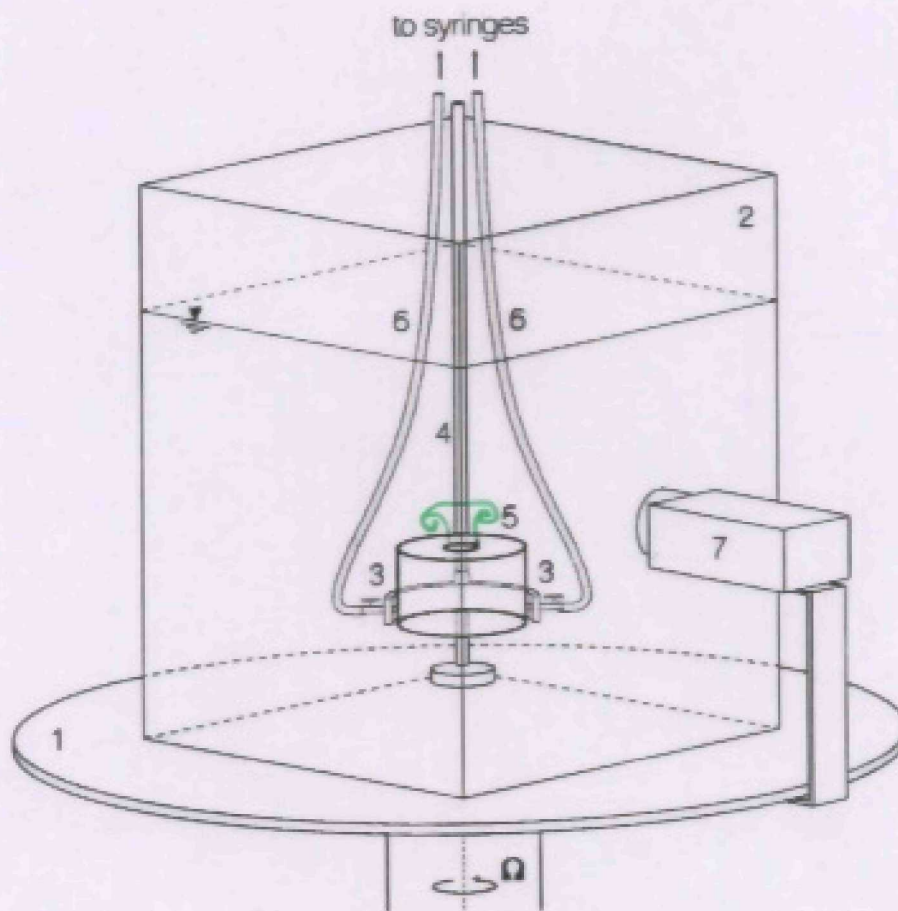


FIGURE 1. Sketch of the experimental apparatus: 1 rotating table, 2 glass tank, 3 fork, 4 stand of the vortex generator 5 cylindrical perspex box with the circular orifice on the top and taps in the lateral surface, 6 plastic tubes connected to the syringes driven by the step-motor system, 7 video-camera. The axis of rotation passes through the centre of the circular orifice.

- Flow visualization
- Particle tracking

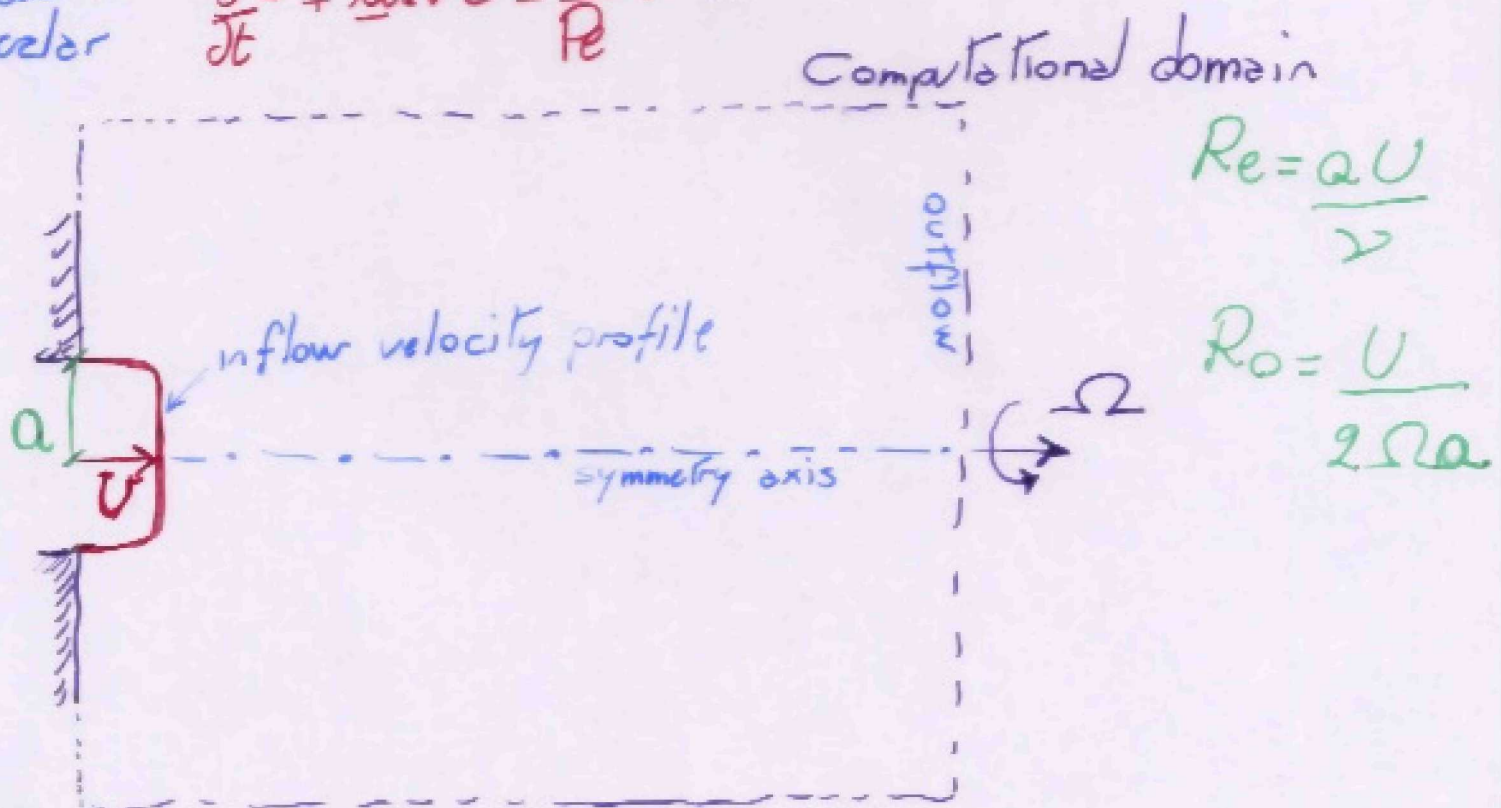
# Numerical Set-up

Direct simulation of 3D  
Navier-Stokes equations in primitive variables

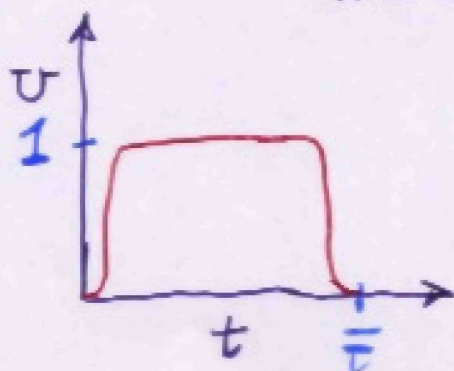
momentum  $\frac{\partial \underline{u}}{\partial t} + \underline{u} \cdot \nabla \underline{u} = -\nabla p + \frac{1}{Re} \nabla^2 \underline{u} - \frac{1}{Ro} \hat{\Omega} \times \underline{u}$

continuity  $\nabla \cdot \underline{u} = 0$

passive scalar  $\frac{\partial C}{\partial t} + \underline{u} \cdot \nabla C = \frac{1}{Re} \nabla^2 C$



Time dependent injection



$L$  injected slug length

$\frac{L}{R} = 1.2$

$\bar{T} \approx 1.3 \frac{R}{U}$

No rotation

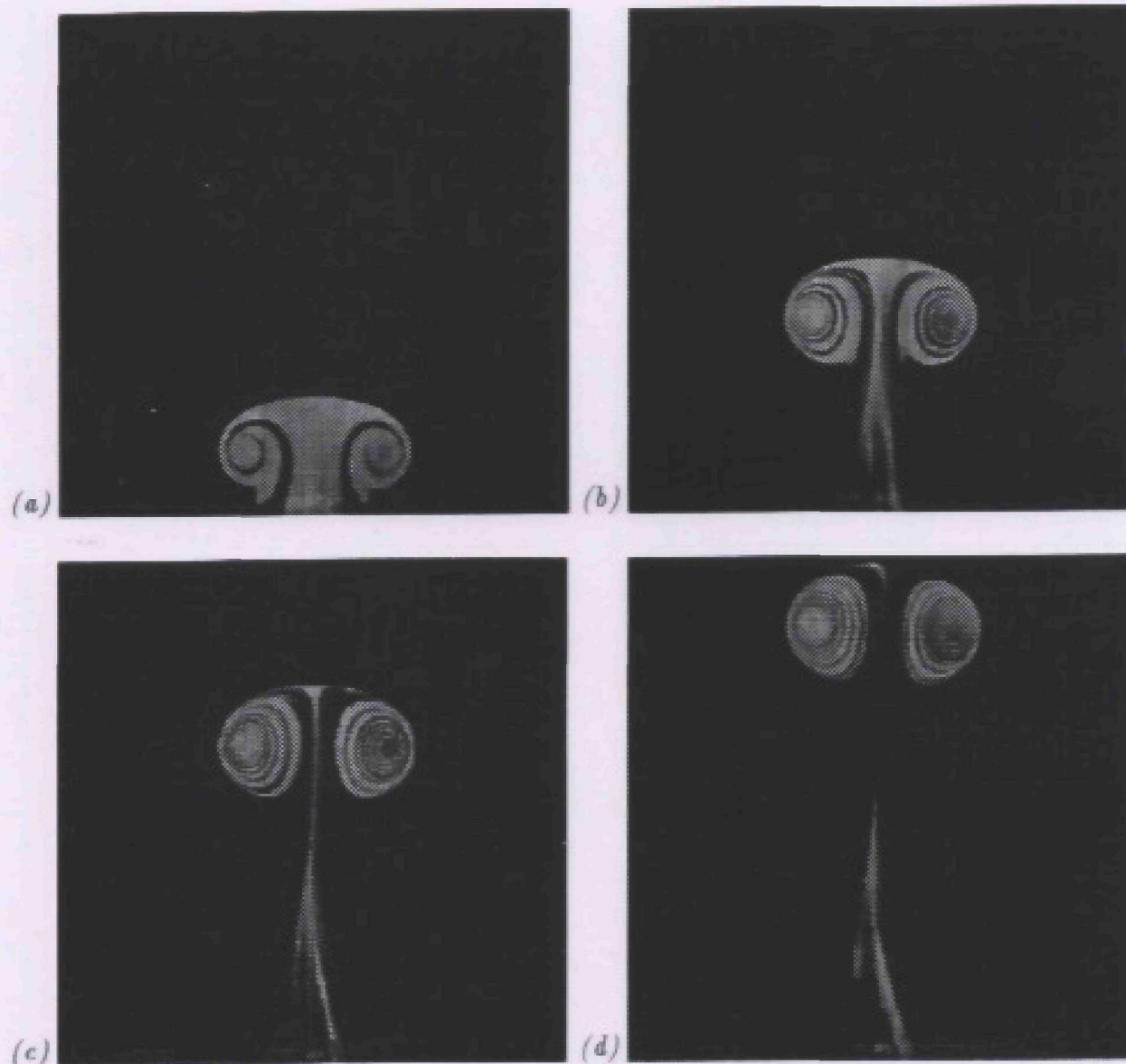


FIGURE 3. Dye-visualizations of a vortex ring evolution at  $Ro = \infty$  and  $Re \simeq 1000$ : (a)  $t = 4$ , (b)  $t = 8$ , (c)  $t = 12$ , (d)  $t = 16$ .

Vortex evolution

The ring translates "steadily" preserving its shape

Rotation  $Ro = 4.8$

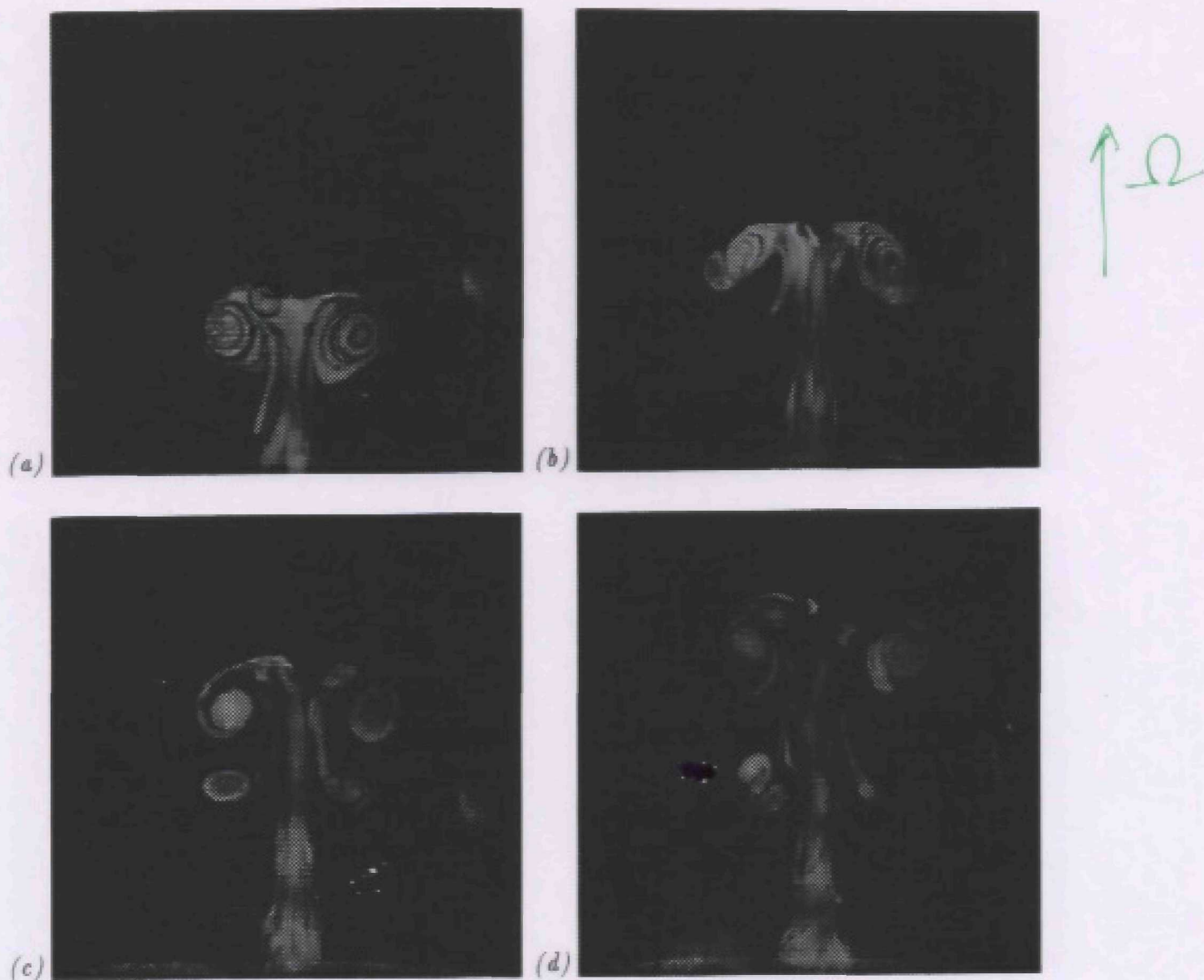
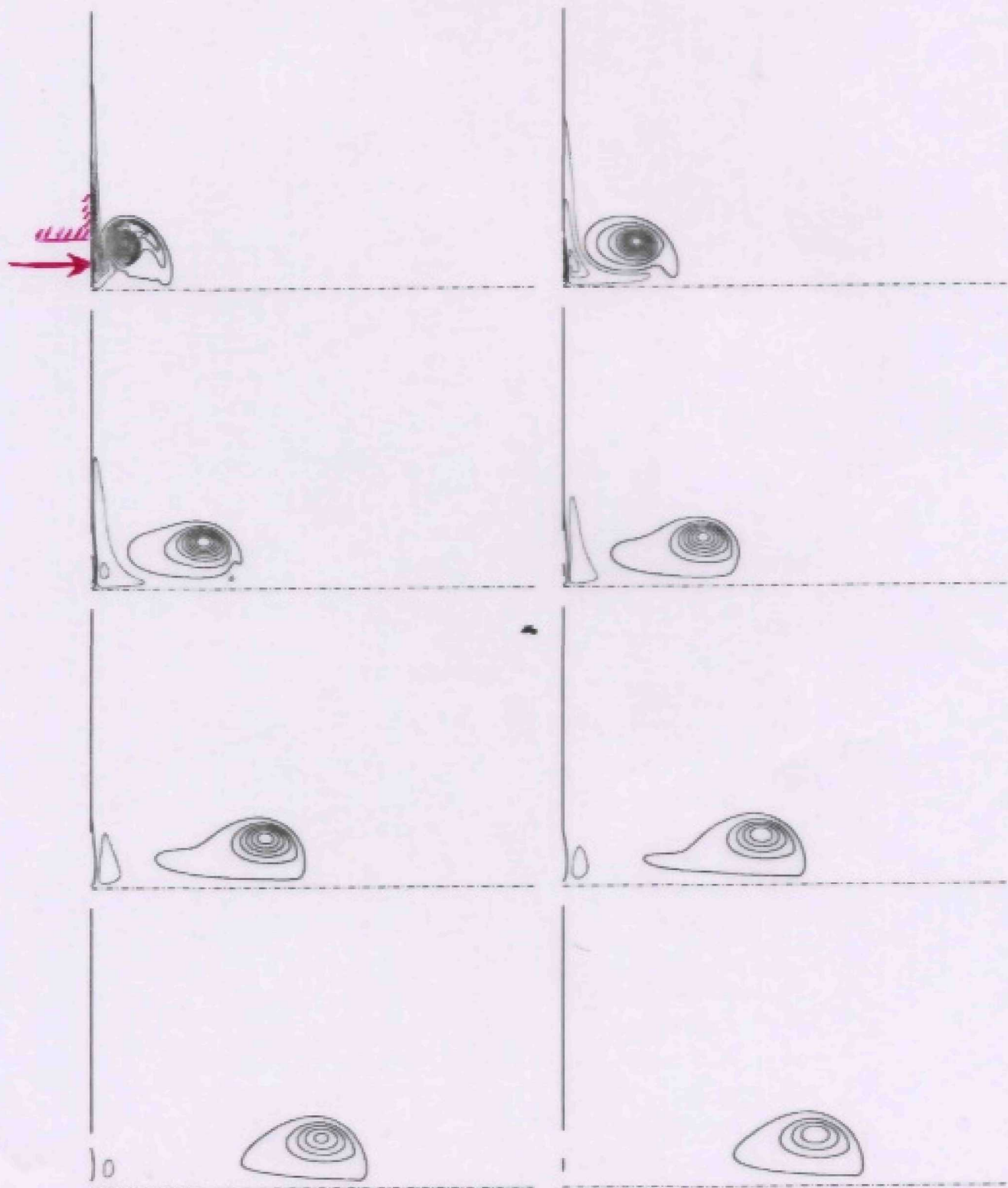


FIGURE 4. Dye-visualizations of a vortex ring evolution at  $Ro = 4.8$  and  $Re \approx 1000$ : (a)  $t = 7$ , (b)  $t = 10$ , (c)  $t = 13$ , (d)  $t = 16$ .

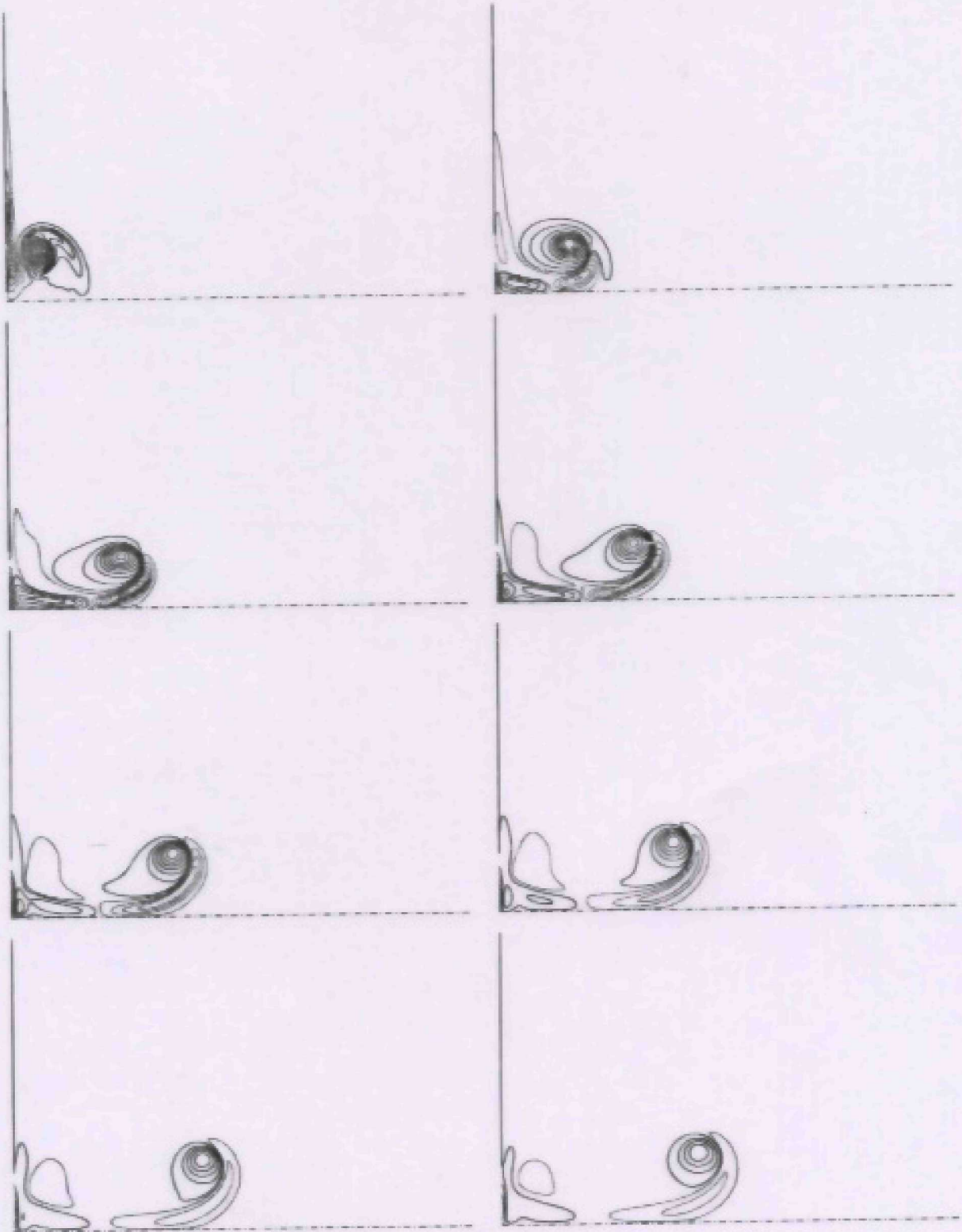
The ring decelerates and secondary structures are shed





Contour plots of azimuthal vorticity at  $Re = 484$  and  $Ro = \infty$  vorticity increments  $\Delta\omega = \pm 0.40$ , — for positive ---- for negative values.

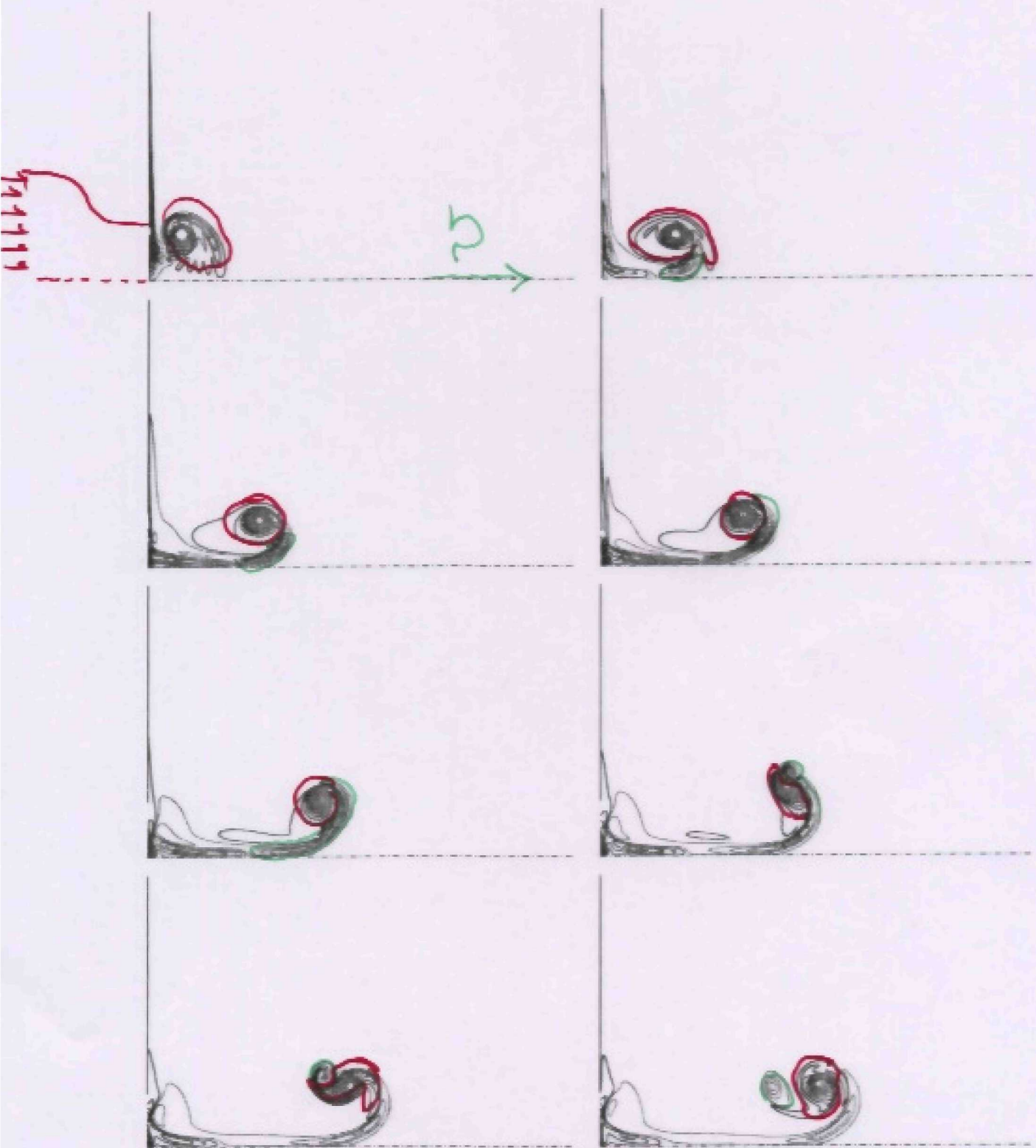
No rotation,  $Ro = \infty$



Contour plots of azimuthal vorticity at  $Re = 484$  and  $Ro = 5.5$  vorticity increments  $\Delta\omega = \pm 0.40$ , — for positive ---- for negative values.

$$Ro = 5.5$$

High Reynolds ( $Re=1500$ )

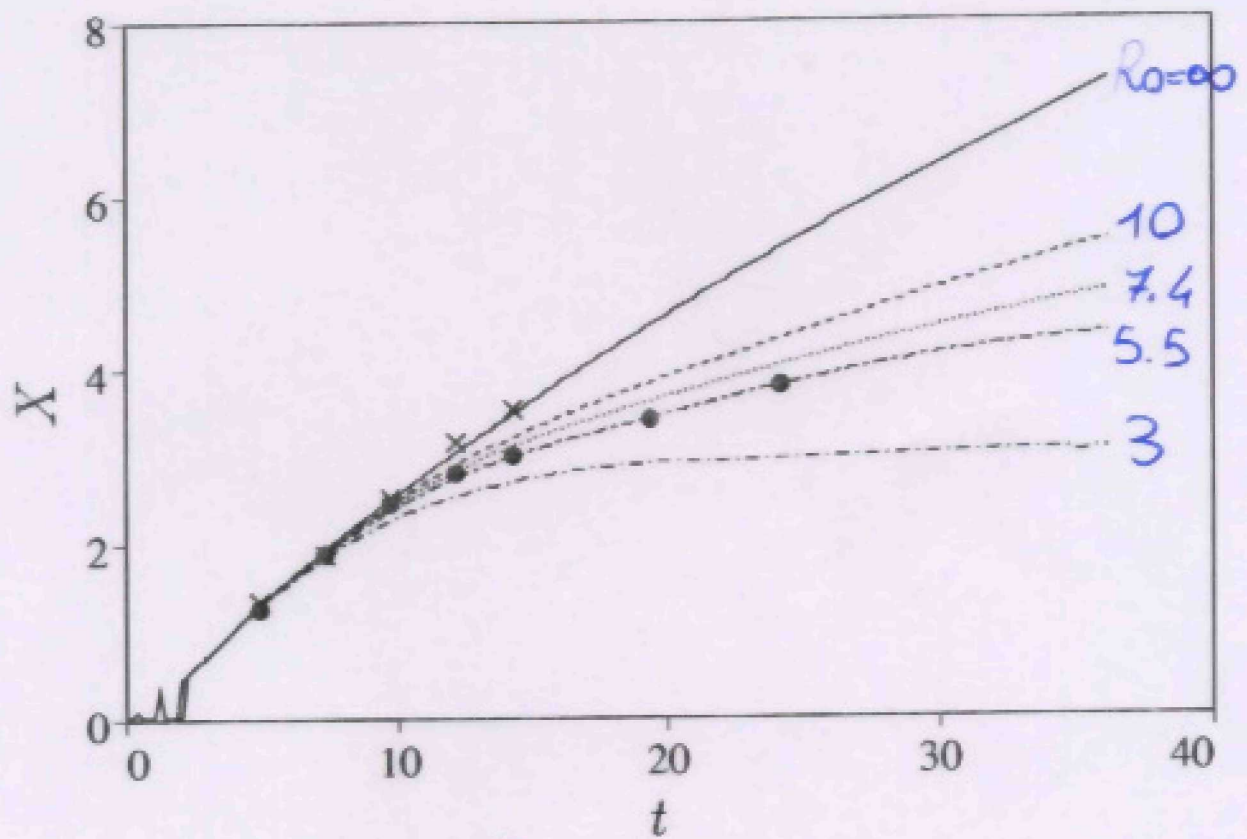


Contour plots of azimuthal vorticity at  $Re=1500$  and  $Ro=10$  vorticity increments  $\Delta\omega = \pm 0.40$ , — for positive ---- for negative values.

- A secondary vortex detaches

# Trajectories

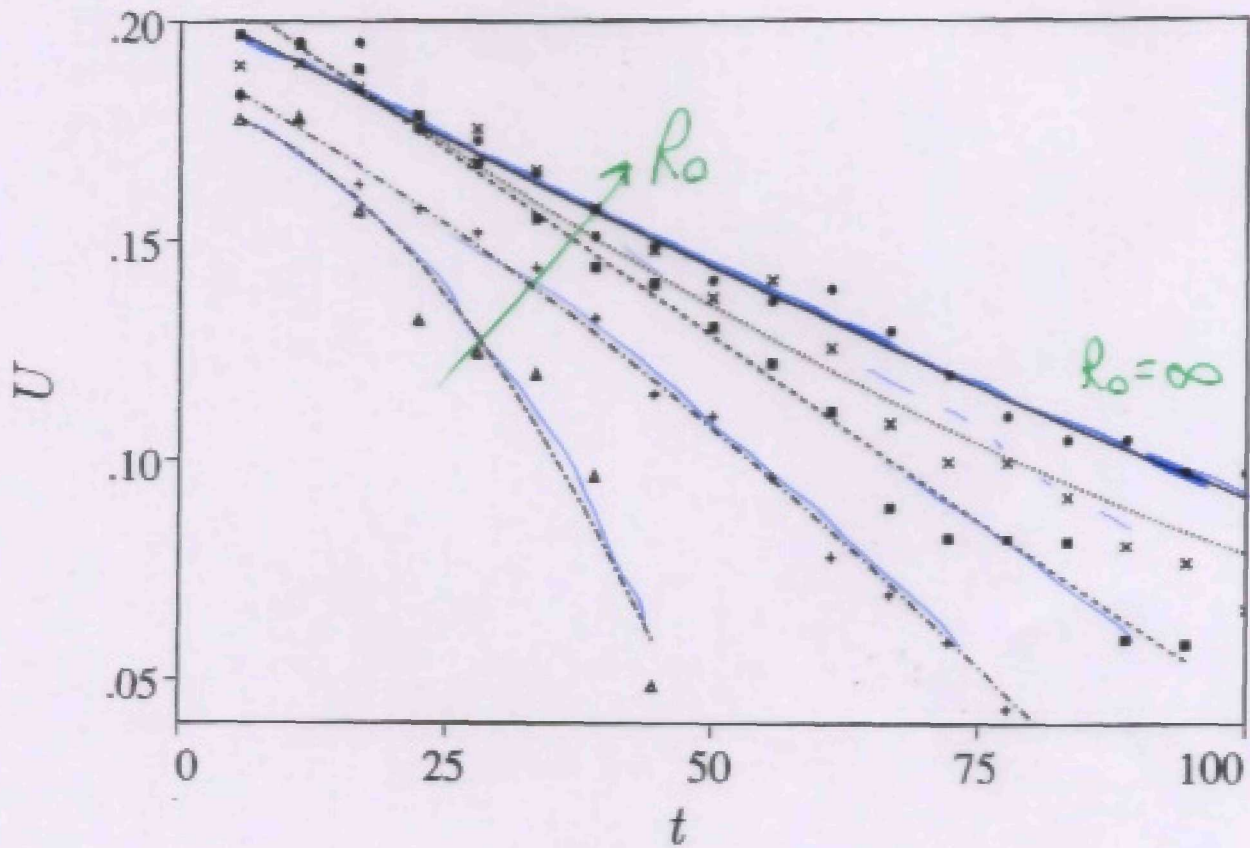
- for higher rotation rates the ring decelerates



x, o experiments

# Ring velocities

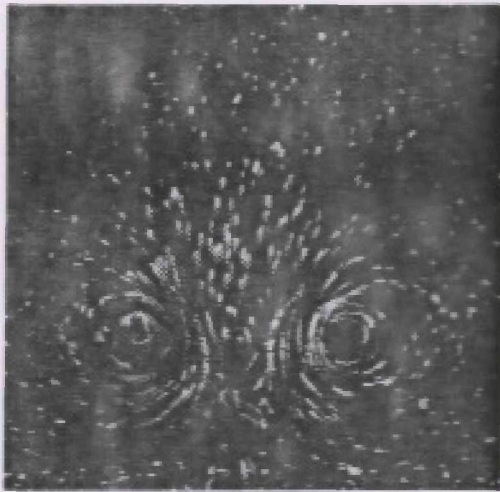
- Translation velocity decreases as  $Ro$  decreases



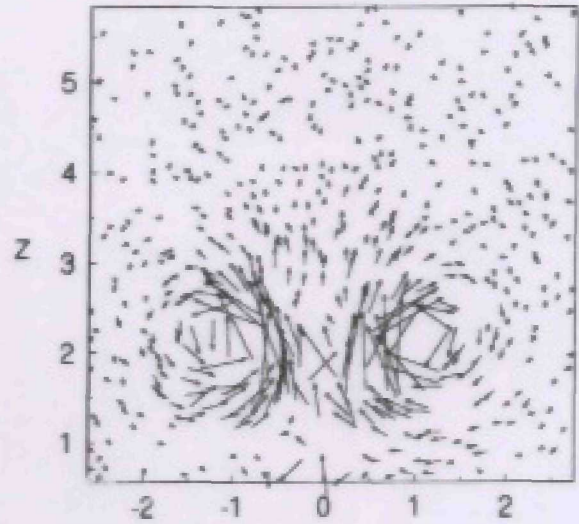
• and — for  $Ro = \infty$ ,  $\times$  and .....  $Ro = 23$ , ■ and ----  $Ro = 15.6$ , + and -·-·-  $Ro = 12.7$ ,  $\nabla$  and ---  $Ro = 8.2$ .

# Particle Tracking

Particle Trajectories



Velocity vectors

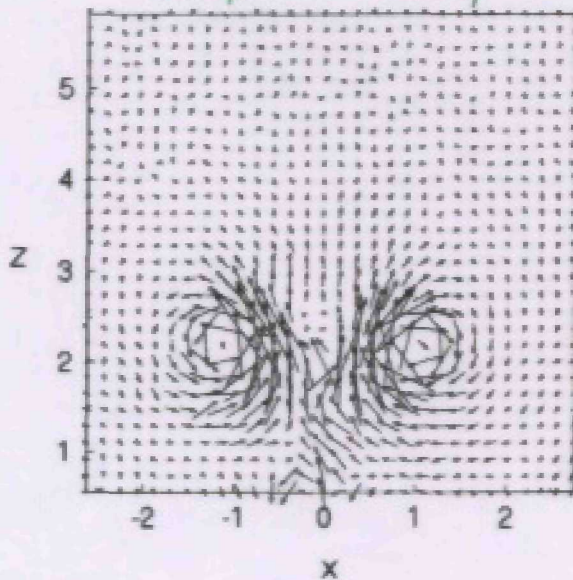


The fluid is seeded by fluorescent particles

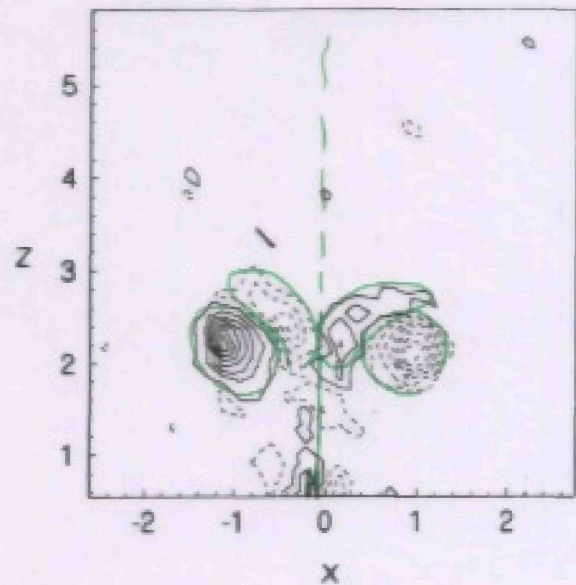
(a)

(b)

Interpolated velocity vectors



vorticity  $\omega = \nabla \wedge \underline{u}$



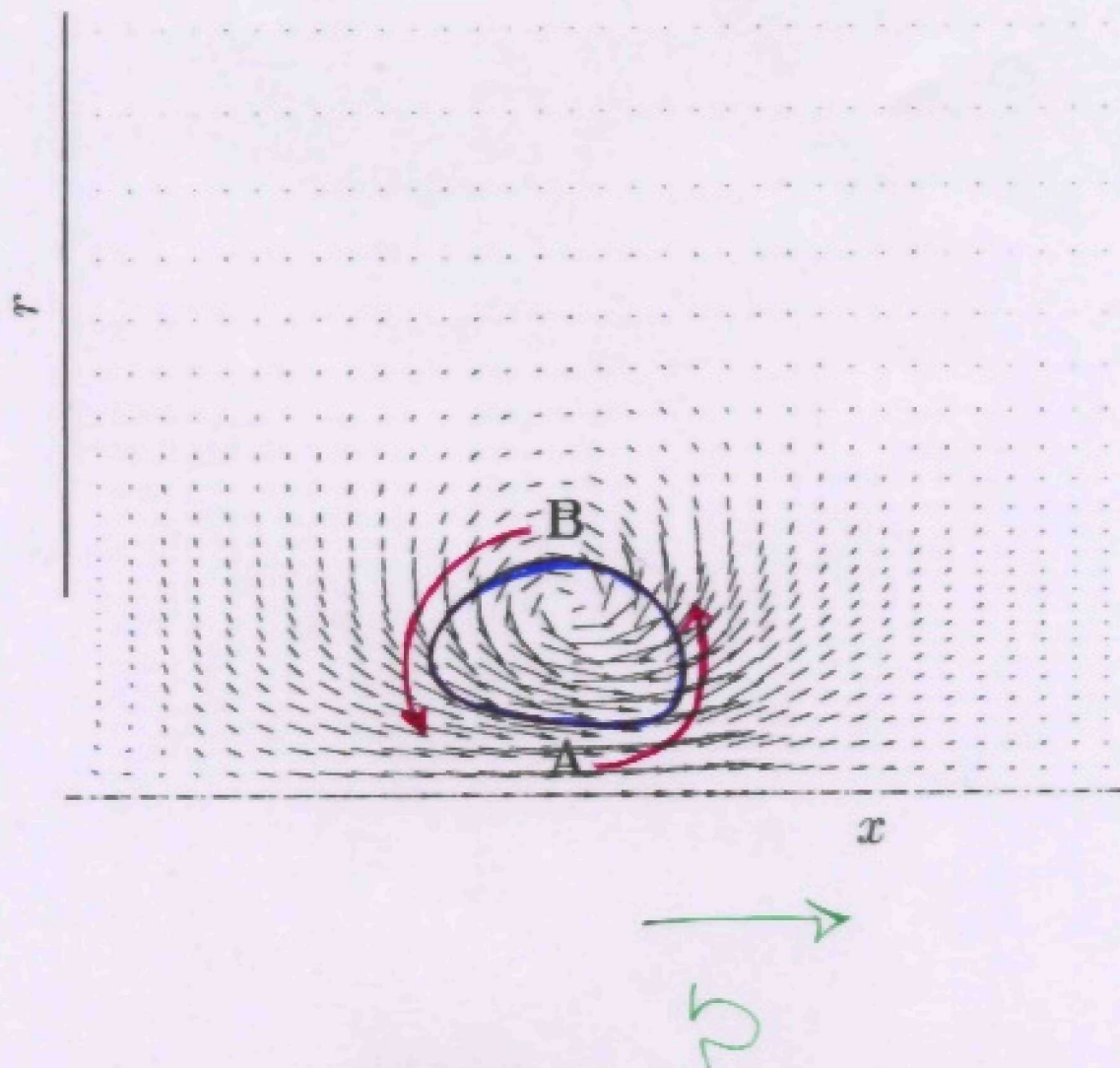
(c)

(d)

FIGURE 8. Particle trajectories (a), measured velocity (b), interpolated velocity (c) and azimuthal vorticity (d), of a vortex ring at  $Ro = 3.5$  and  $Re = 484$  and  $t = 6$ . Vorticity increments  $\Delta\omega = 0.5$ , — for positive and ..... for negative values.  $X \equiv r$  for  $X > 0$  and  $X \equiv -r$  for  $X < 0$ .

## Rotation effects

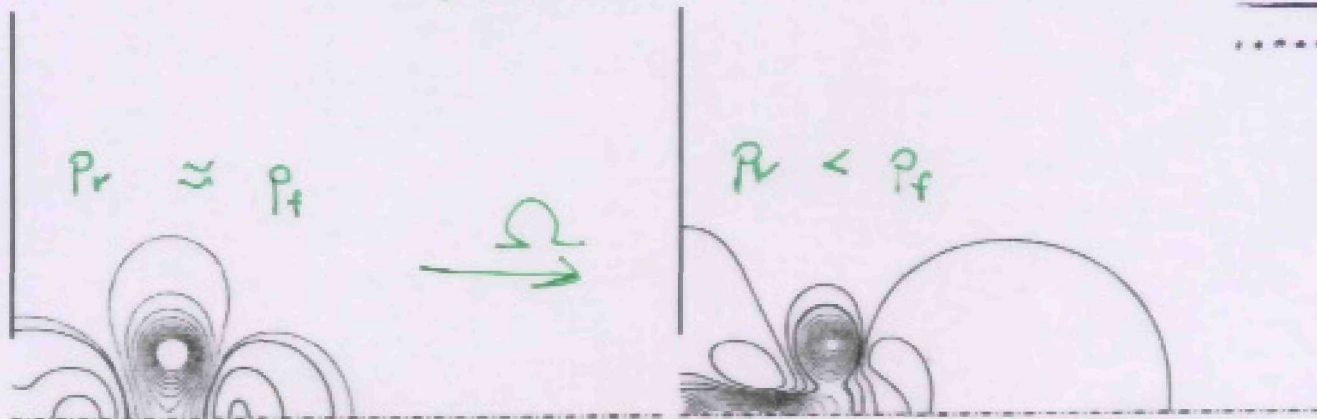
- the ring slows down and cross-diffusion weakens the structures.
- an oppositely-signed vortex ring forms ahead of the primary ring.



# Pressure

- Anticyclone  $\Rightarrow$  'high pressure'
- Cyclone  $\Rightarrow$  'low pressure'

Pressure



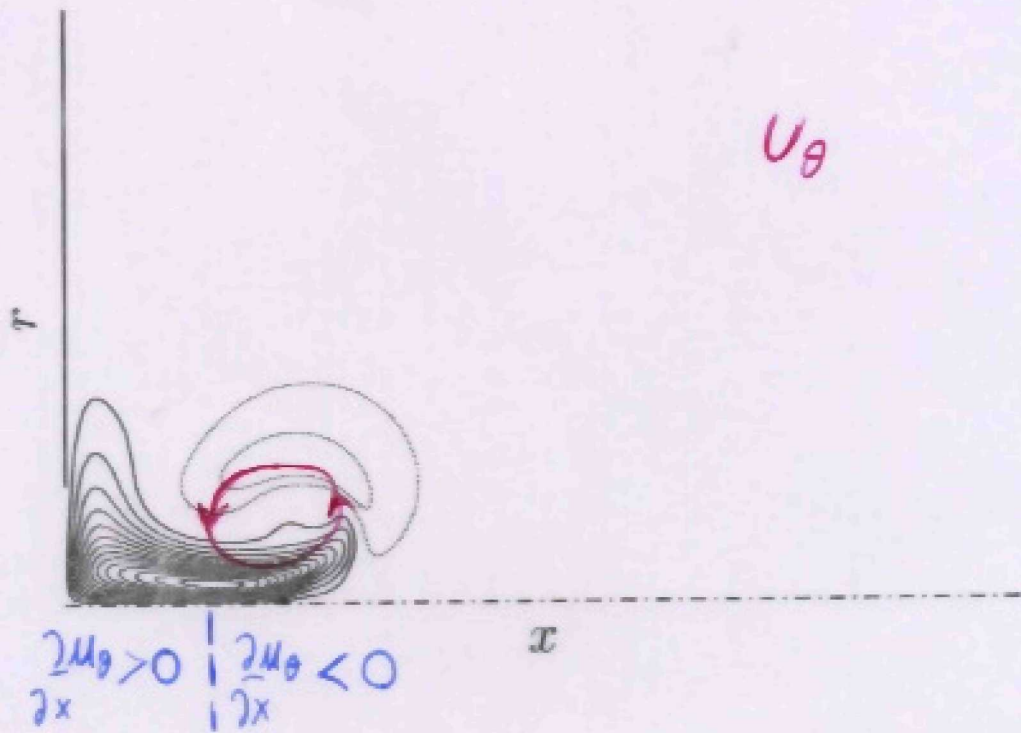
$Ro = \infty$

$Ro = 5.5$

"Dye"



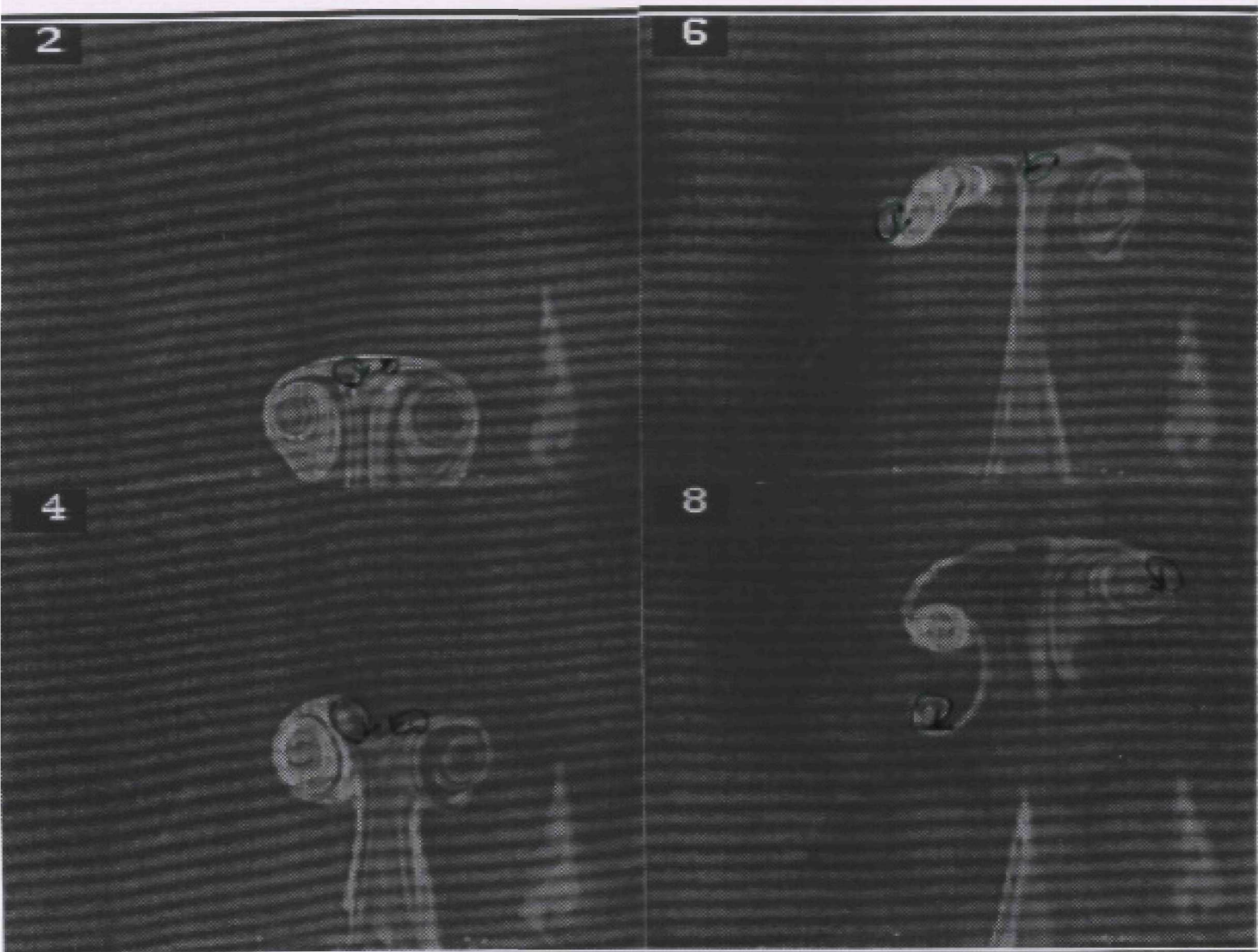




$$\frac{\partial \omega_\theta}{\partial t} + \mathbf{u} \cdot \nabla \omega |_\theta = \omega \cdot \nabla \mathbf{u} |_\theta + \frac{1}{\text{Ro}} \frac{\partial u_\theta}{\partial x} + \frac{1}{\text{Re}} \nabla^2 \omega |_\theta$$

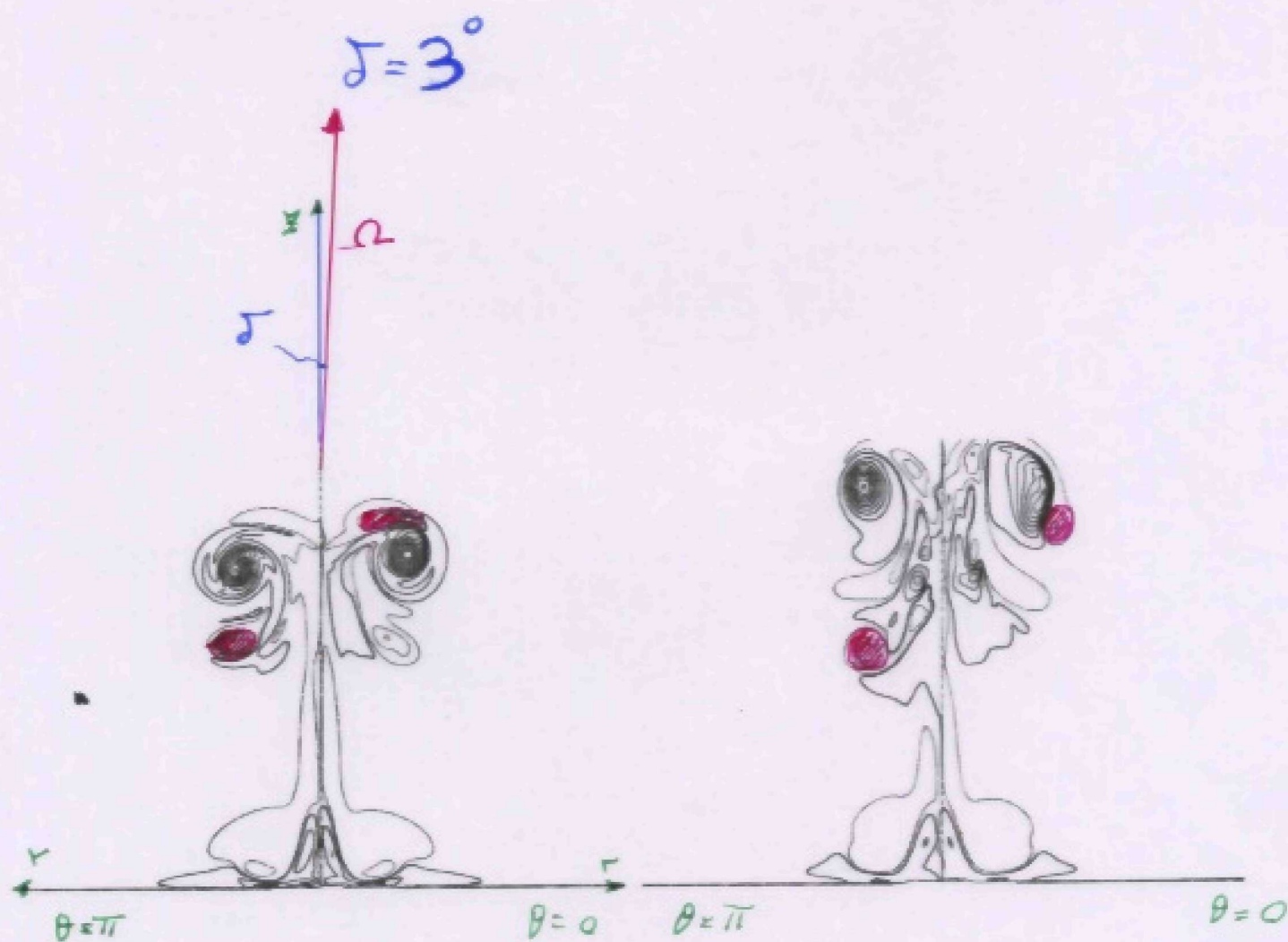


# 3D phenomena



- experimental evidence of asymmetry
- no Widnall instability

- small misalignment between axis of rotation and propagation of the vortex



$$\Omega_z = \Omega \cos(\delta) \approx \Omega$$

$$\Omega_r = \Omega \sin(\delta) \cos(\theta) \approx \delta \Omega \cos(\theta)$$

# High Rotations

$$Ro \leq 1$$

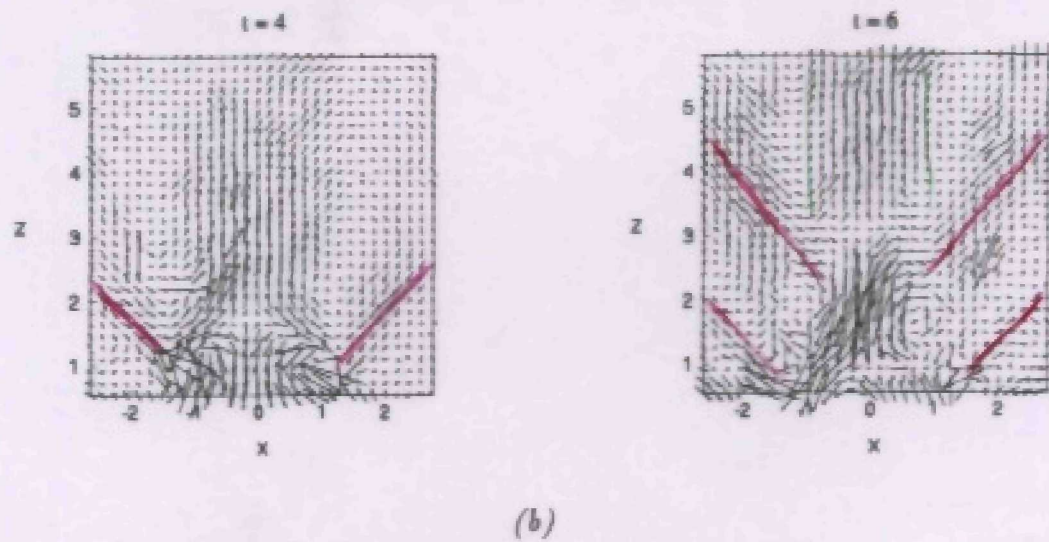
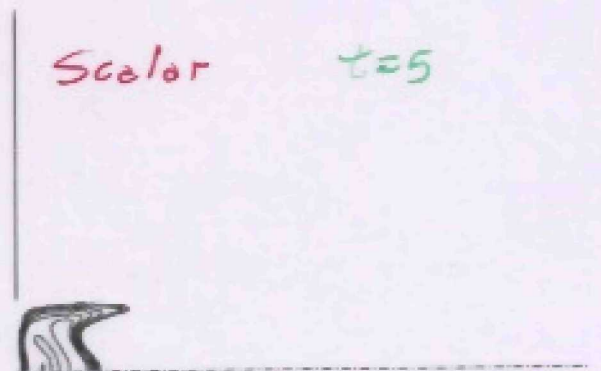
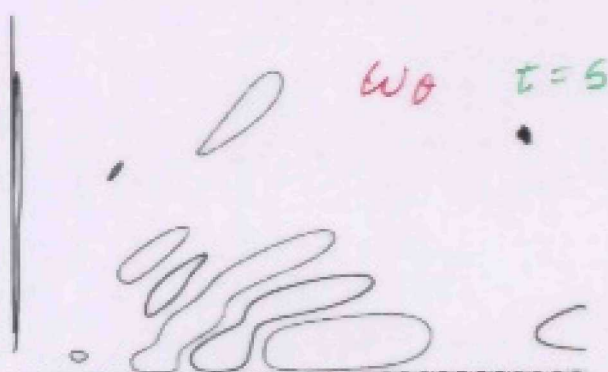
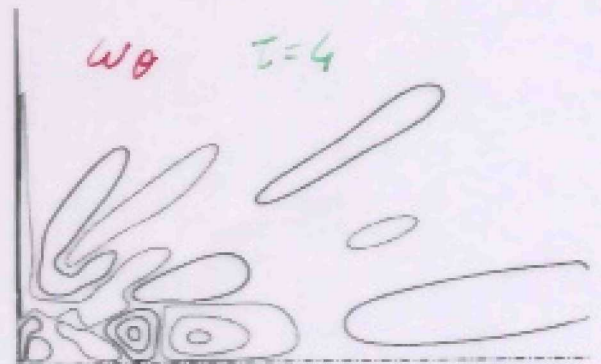
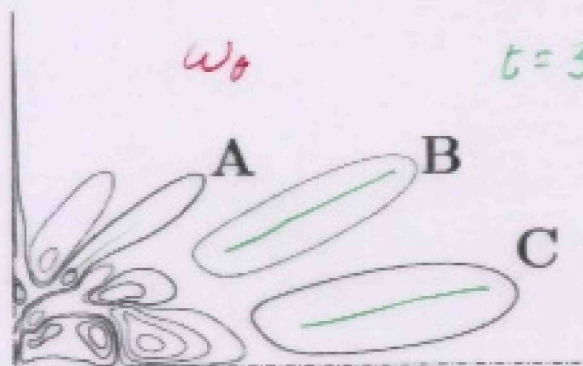
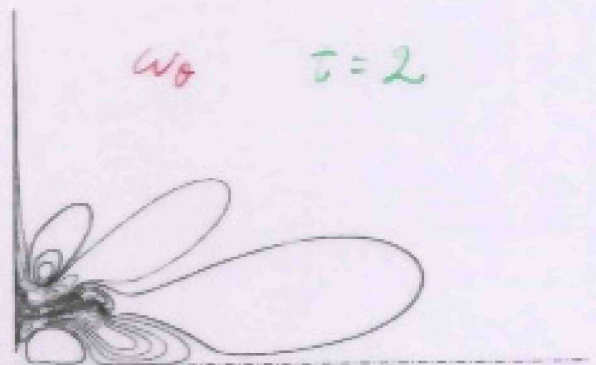
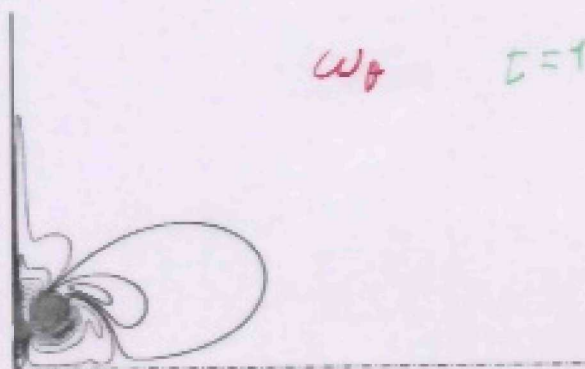


FIGURE 14. Interpolated velocity field of a vortex ring at  $Ro = 0.605$  and  $Re = 484$ : (a)  $T = 4$ , (b)  $T = 6$ .

- no ring formation
- inclined shear-layers

## High rotations

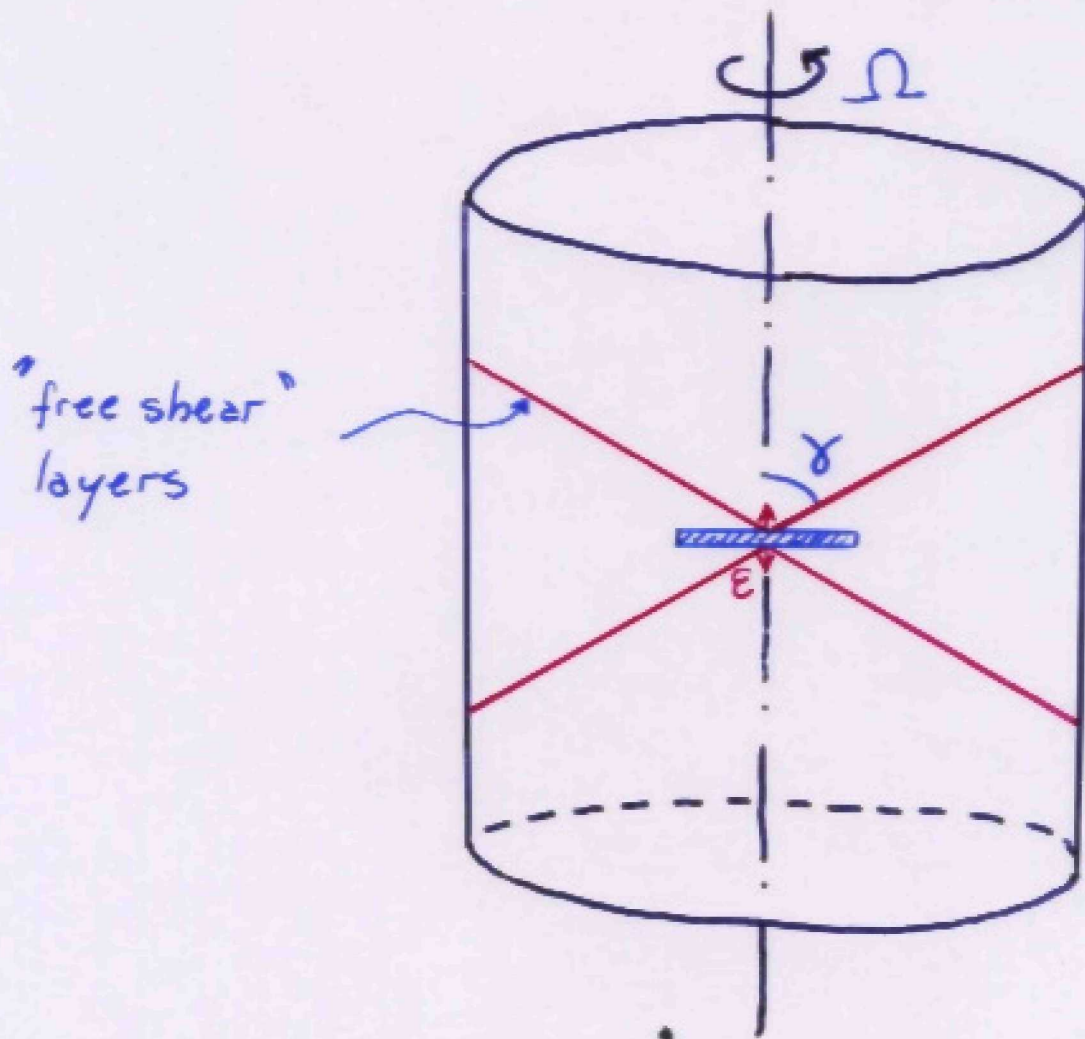
- the ring does not form



- inclined shear layers as for the problem of 'oscillating disk' (Greenspan, 1968).

$$Re = 484 \quad Ro = 0.6$$

# Oscillating disk (Greenspan, 1968)



The disk performs 'infinitesimal' oscillations  
 $\epsilon(t) = \epsilon_0 \sin(f^* t)$

$$\text{if } 2\Omega \gg f^* \quad \gamma = \sin^{-1}(f^*/2\Omega)$$

# Steady, infinitesimal forcing

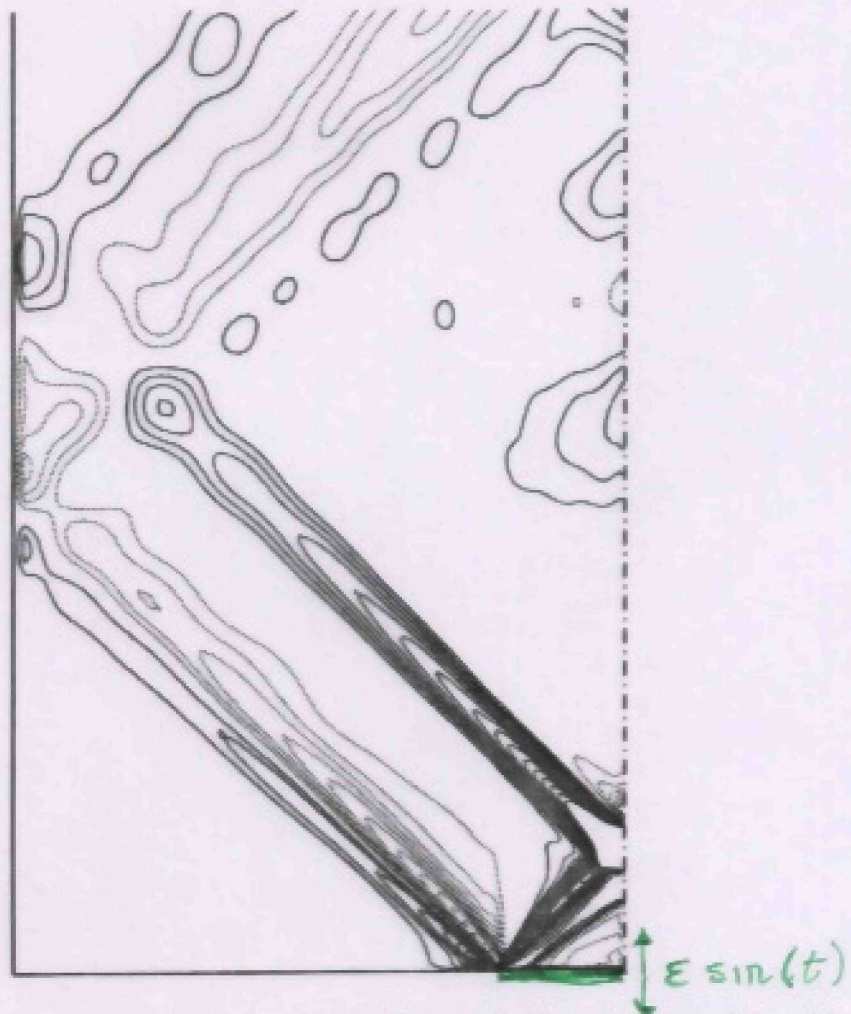


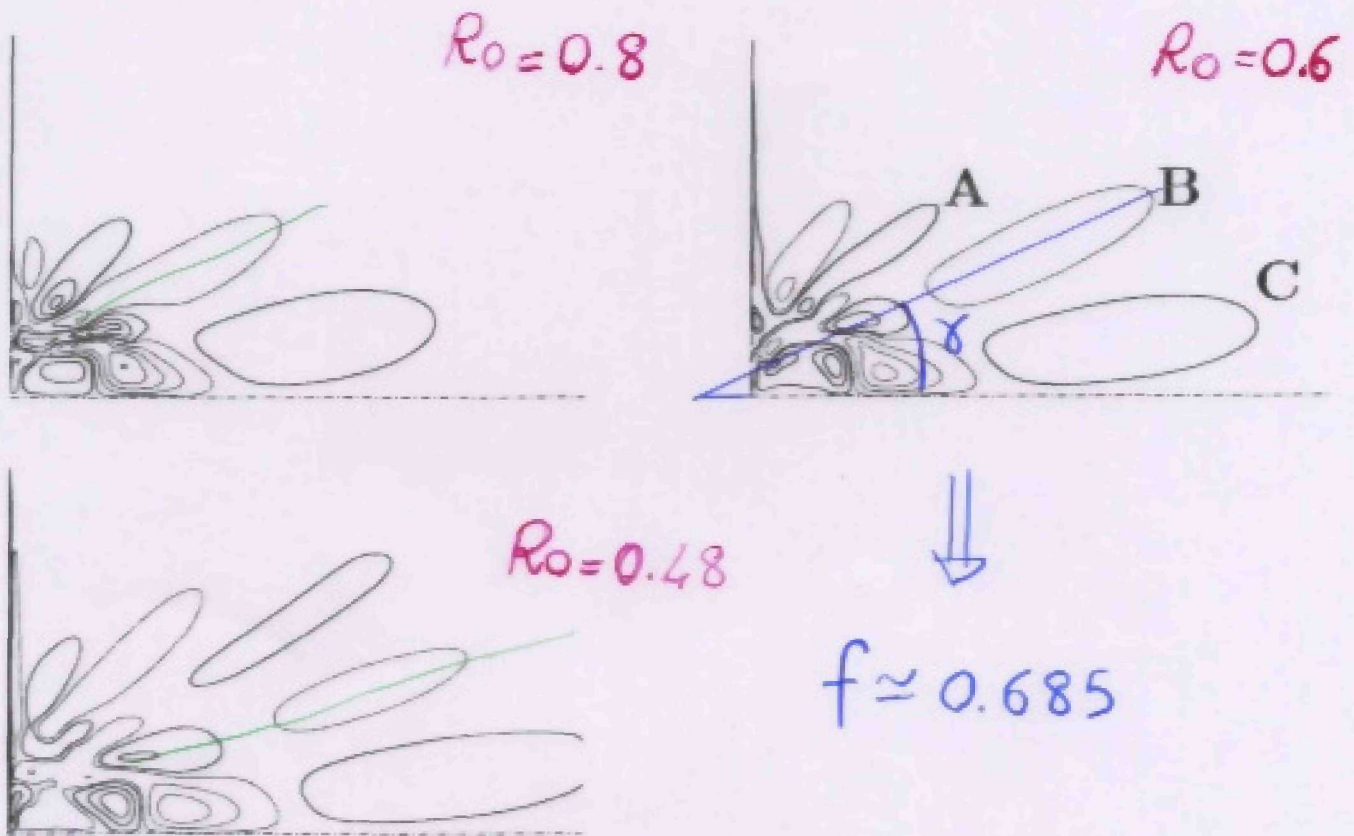
FIGURE 17. Contour plots of azimuthal vorticity at  $Re = 484$ ,  $Ro = 0.707$  and  $t = 10\pi$ . Vorticity increments  $\Delta\omega = \pm 0.01$ , — for positive, ---- for negative values.

$$f = 1 \quad Ro = \frac{\sqrt{2}}{2} \implies \gamma = 45^\circ$$

$t = \text{const}$

•  $\gamma = \sin^{-1}(Ro f)$

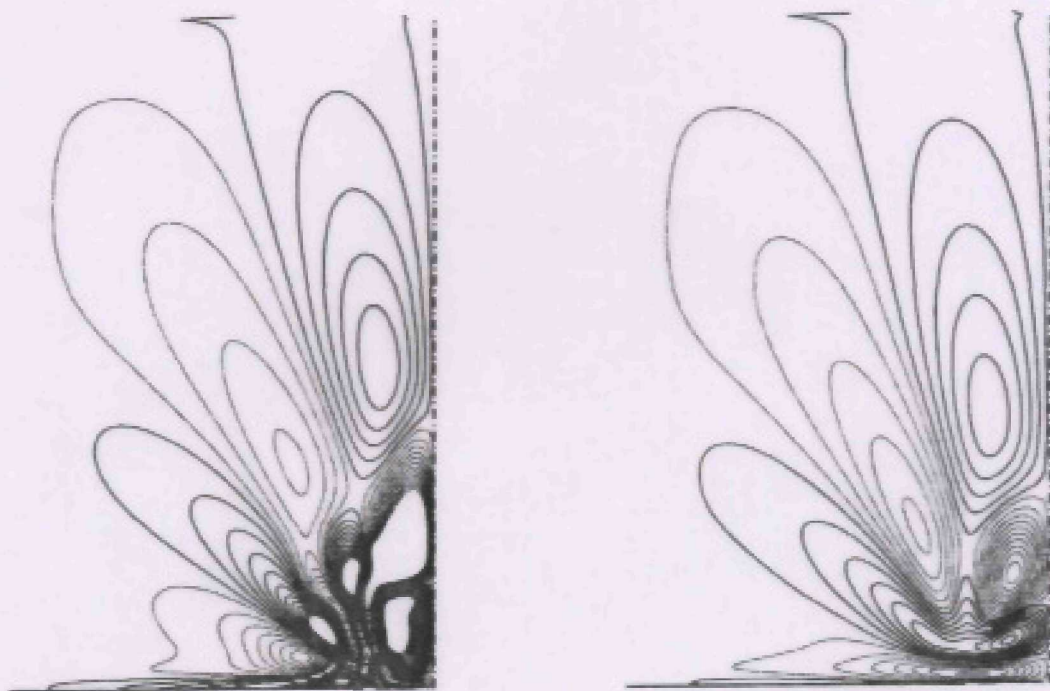
$f$  calculated from a simulation



	$\gamma$ (predicted)	$\gamma$ (measured)
$Ro = 0.8$	$33^\circ$	$30^\circ$
$Ro = 0.48$	$19.5^\circ$	$19^\circ$

• The same agreement for 'A' and 'C' structures





(a) Non-linear

(b) Linear

FIGURE 16. Contour plots of azimuthal vorticity at  $Re = 484$ ,  $Ro = 0.707$  and  $t = 7.2$ : (a) full Navier-Stokes run, (b) linear run. Vorticity increments  $\Delta\omega = \pm 0.05$ , — for positive, ---- for negative values.

• Shear-layers due to linear dynamics

Transient (impulsive) forcing  $\Rightarrow$

- many angles of the structures
- angles diminishes in time

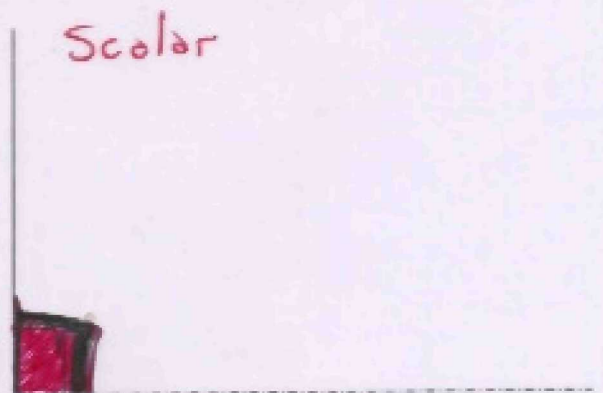
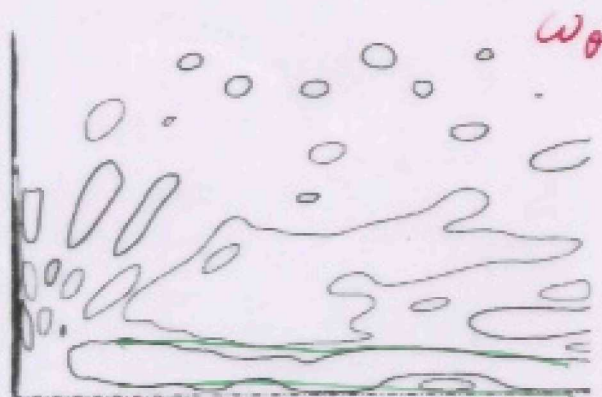
## 'Very high' rotations

- $Ro \rightarrow 0$

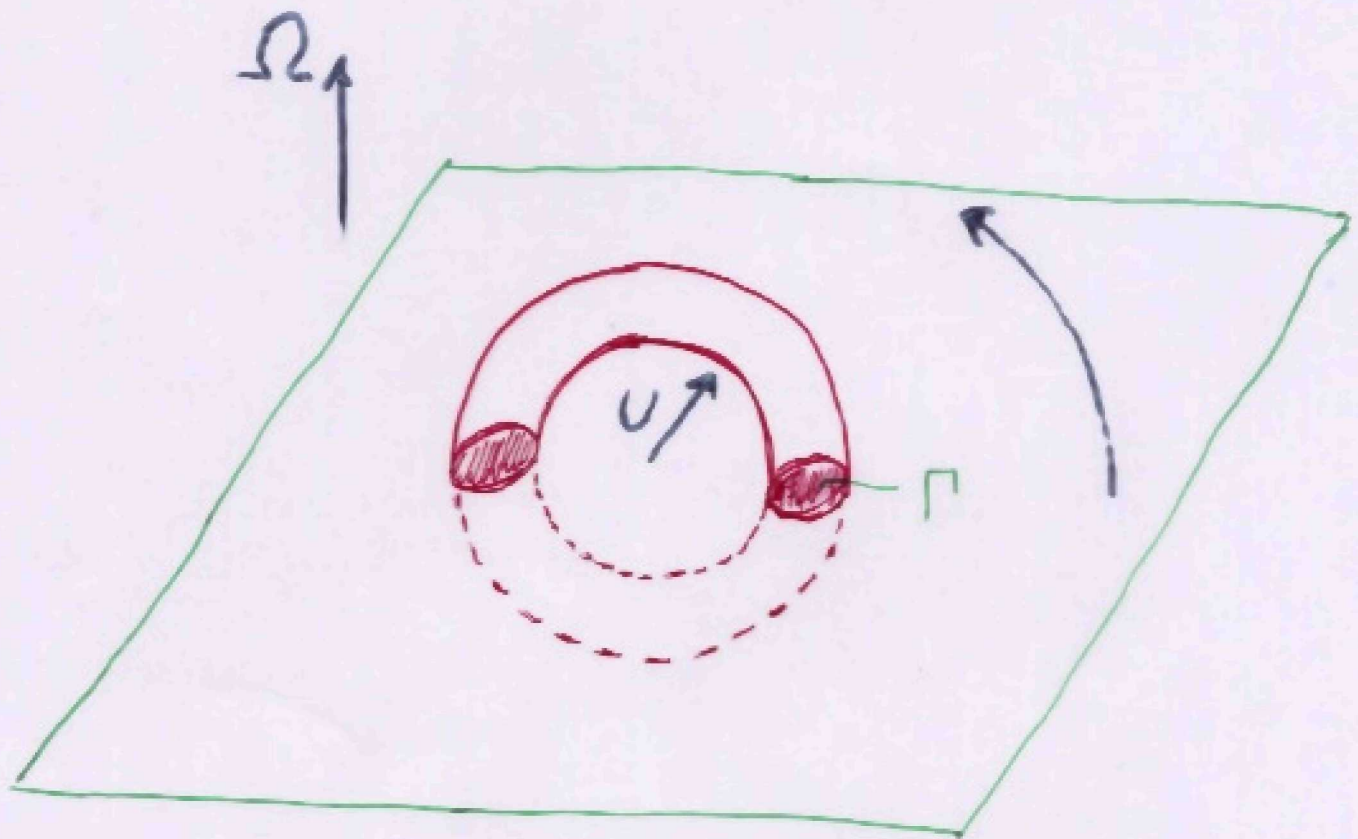
$$\frac{\partial \omega_\theta}{\partial t} + \mathbf{u} \cdot \nabla \omega |_\theta = \omega \cdot \nabla \mathbf{u} |_\theta + \frac{1}{Ro} \frac{\partial u_\theta}{\partial x} + \frac{1}{Re} \nabla^2 \omega |_\theta,$$

- $\rightarrow \partial u_\theta / \partial x = 0$

'two dimensional' Taylor-Proudman column



$$Ro \approx 0.1$$



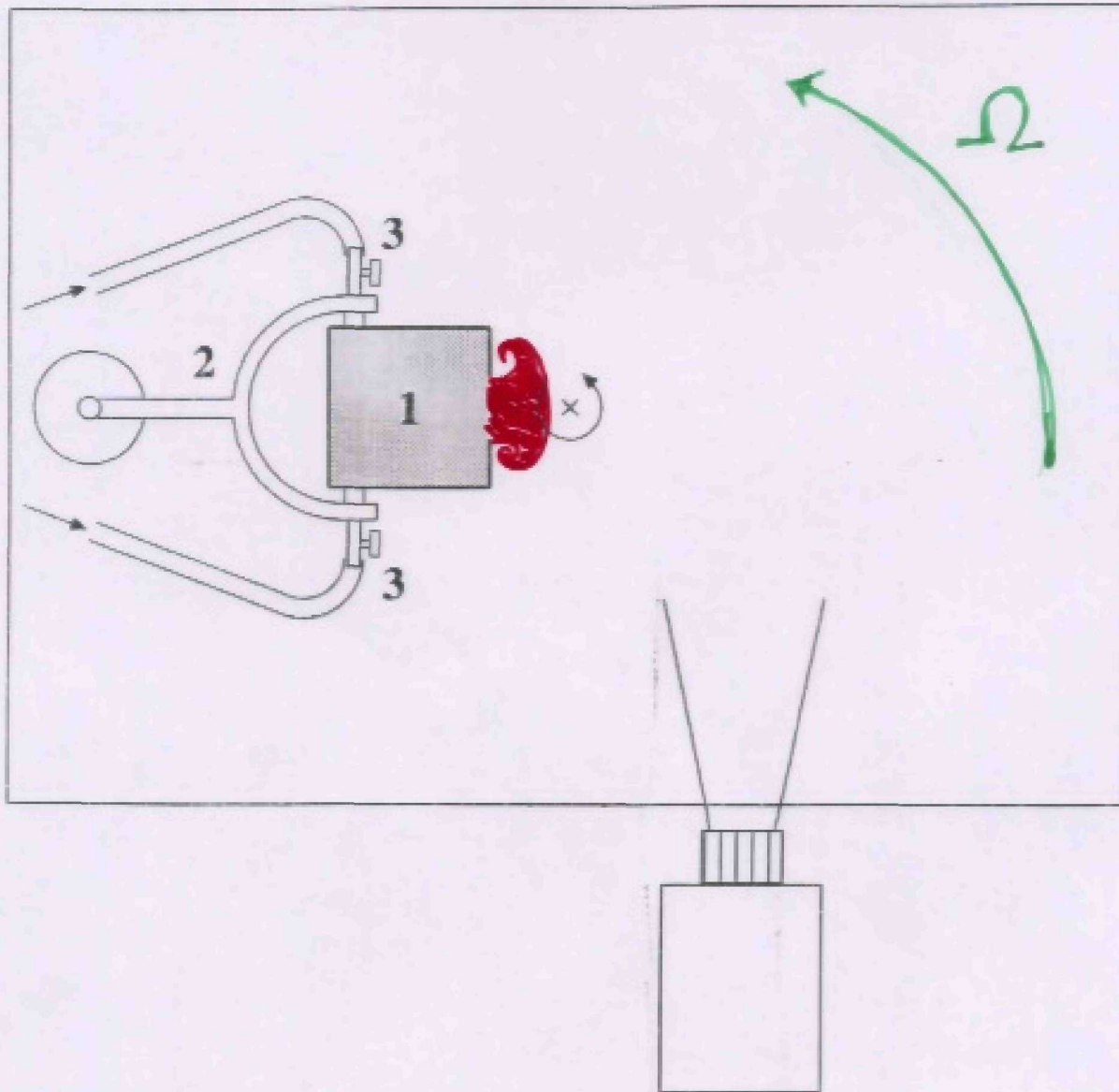
$$R_e = \Gamma / \nu$$

$$R_o = \Gamma / 2\Omega R^2$$

$\Gamma$  = ring circulation.

$R$  = ring radius

## Experimental set-up



Vortex ring generator **1**, fork and stand **2**,  
watertaps and pipes **3**,

# Initial Conditions

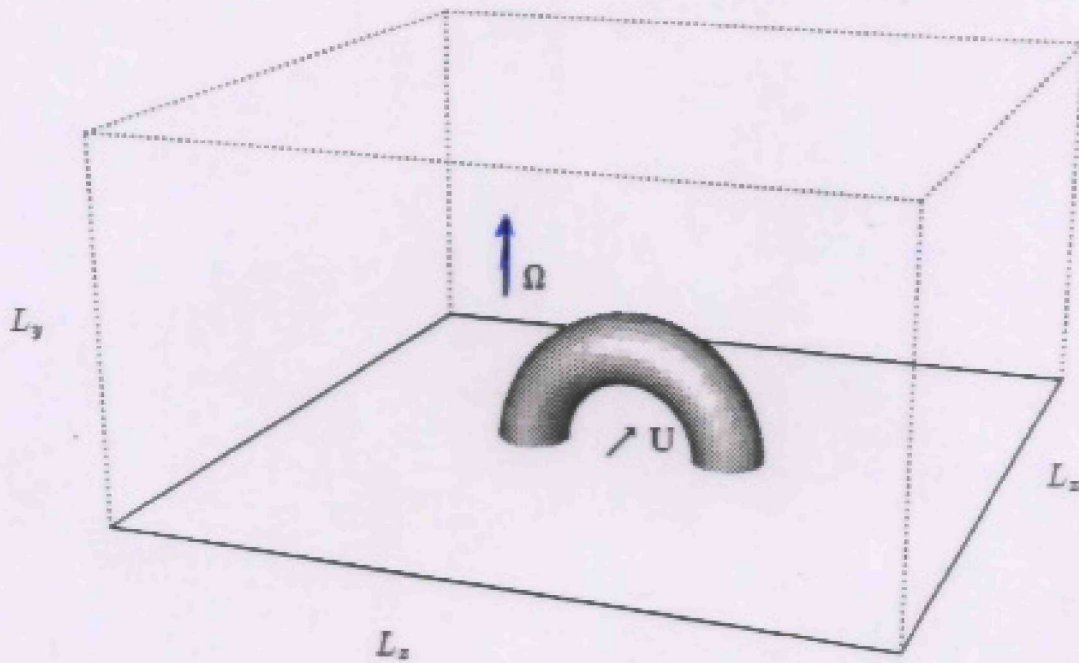
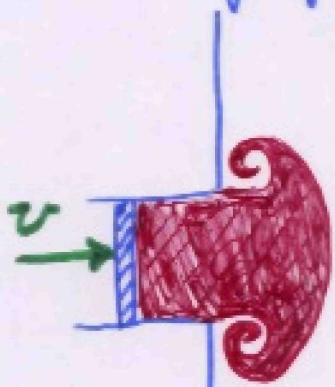


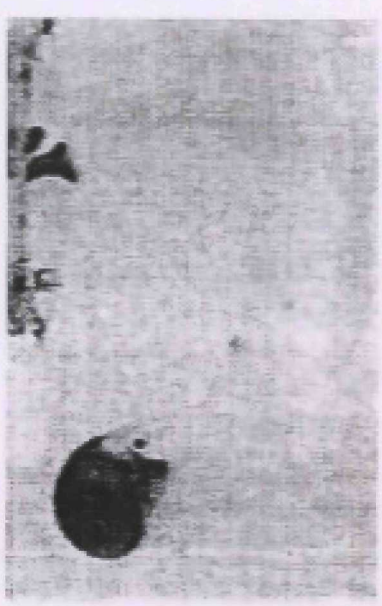
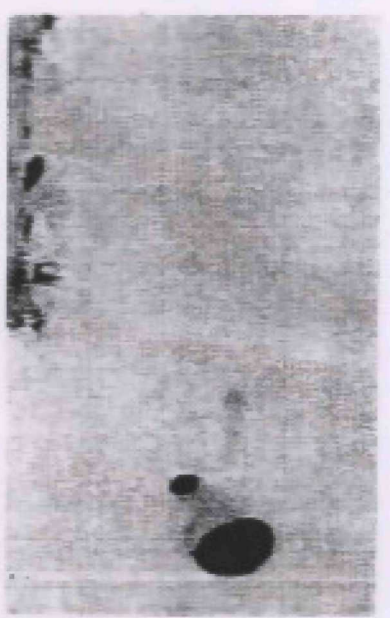
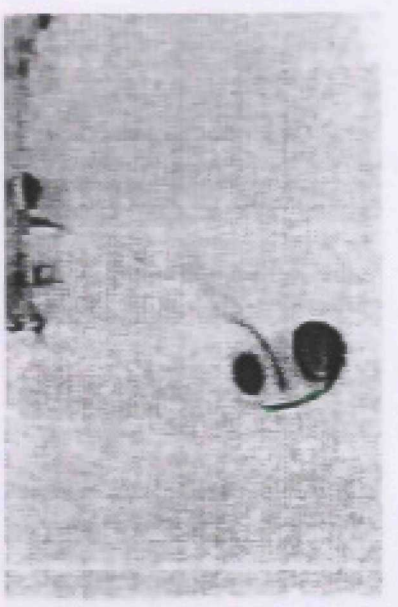
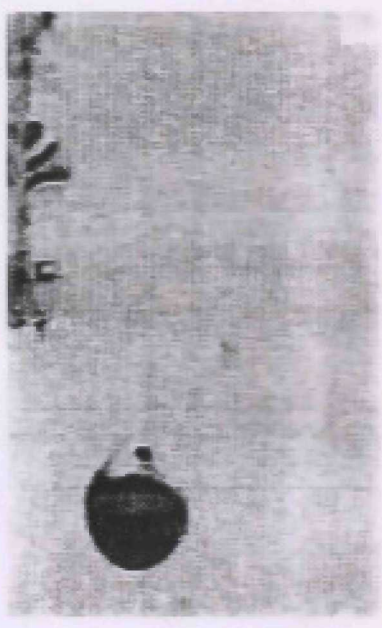
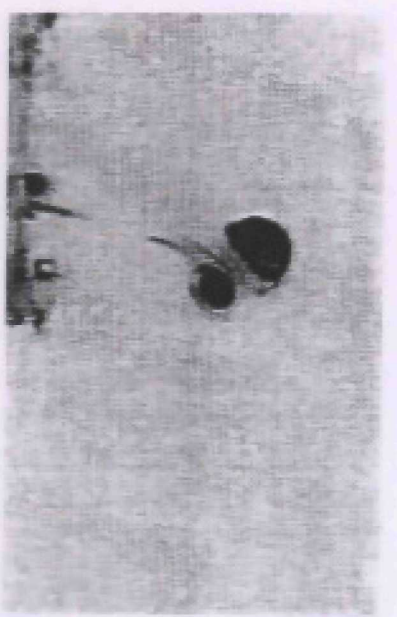
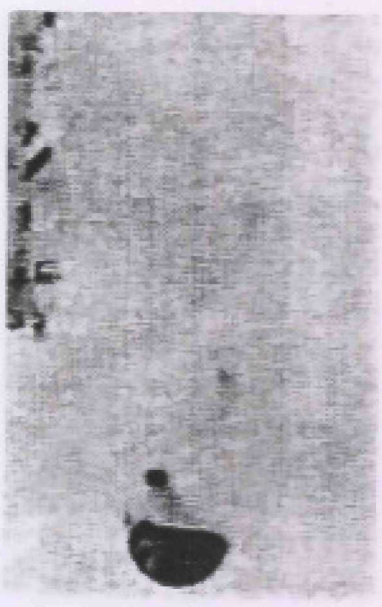
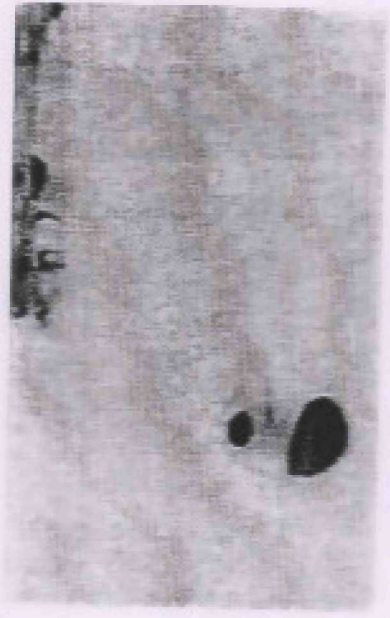
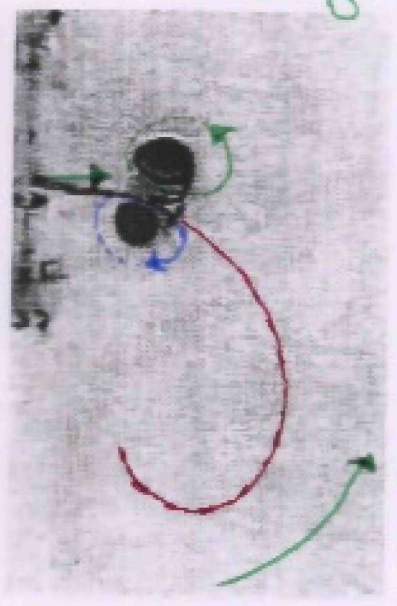
FIGURE 2. Schematic of the initial condition and computational box.

vortex ring such to match the experimental ring generation



only half ring was simulated

$Re \approx 900$   
 $Ro = 10$



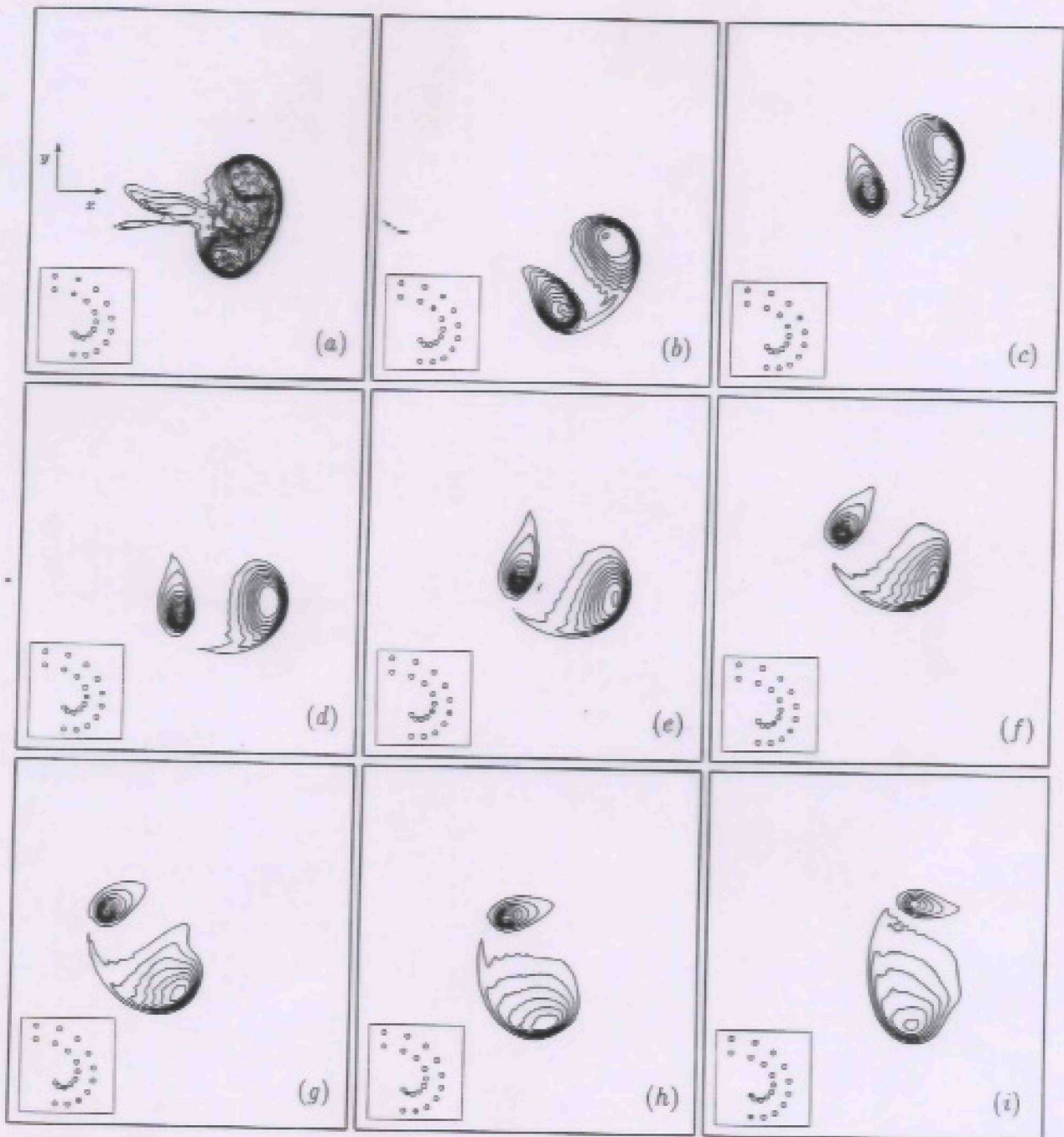


FIGURE 13: Contour plots of passive scalar concentration  $C$  in the horizontal symmetry plane  $z = 0$  of the vortex ring, obtained from a numerical simulation with  $\bar{R}i_0 = 20$  and  $Ri_c = 300$ . (a)  $t = 17$ , (b)  $t = 53$ , (c)  $t = 50$ , (d)  $t = 67$ , (e)  $t = 83$ , (f)  $t = 100$ , (g)  $t = 117$ , (h)  $t = 133$ , (i)  $t = 150$ . Contour increments  $\Delta C = 0.1$ ; minimum contour levels: (a-c)  $C = 0.25$ , (d)  $C = 0.2$  and (e-i)  $C = 0.15$ . The insets show the trajectories of the core centres, the instantaneous position of the vortex ring in each panel is denoted by black dots.

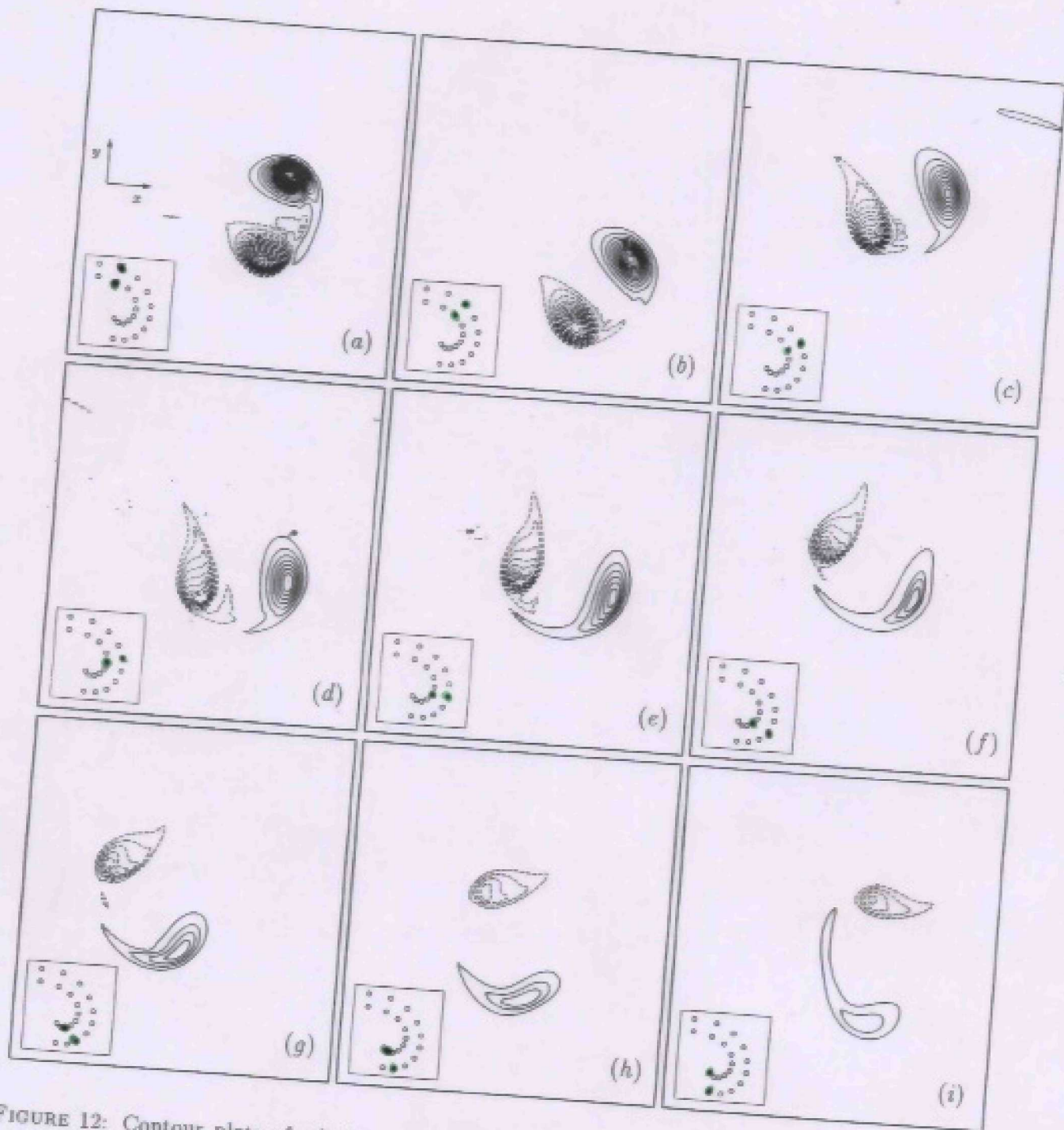
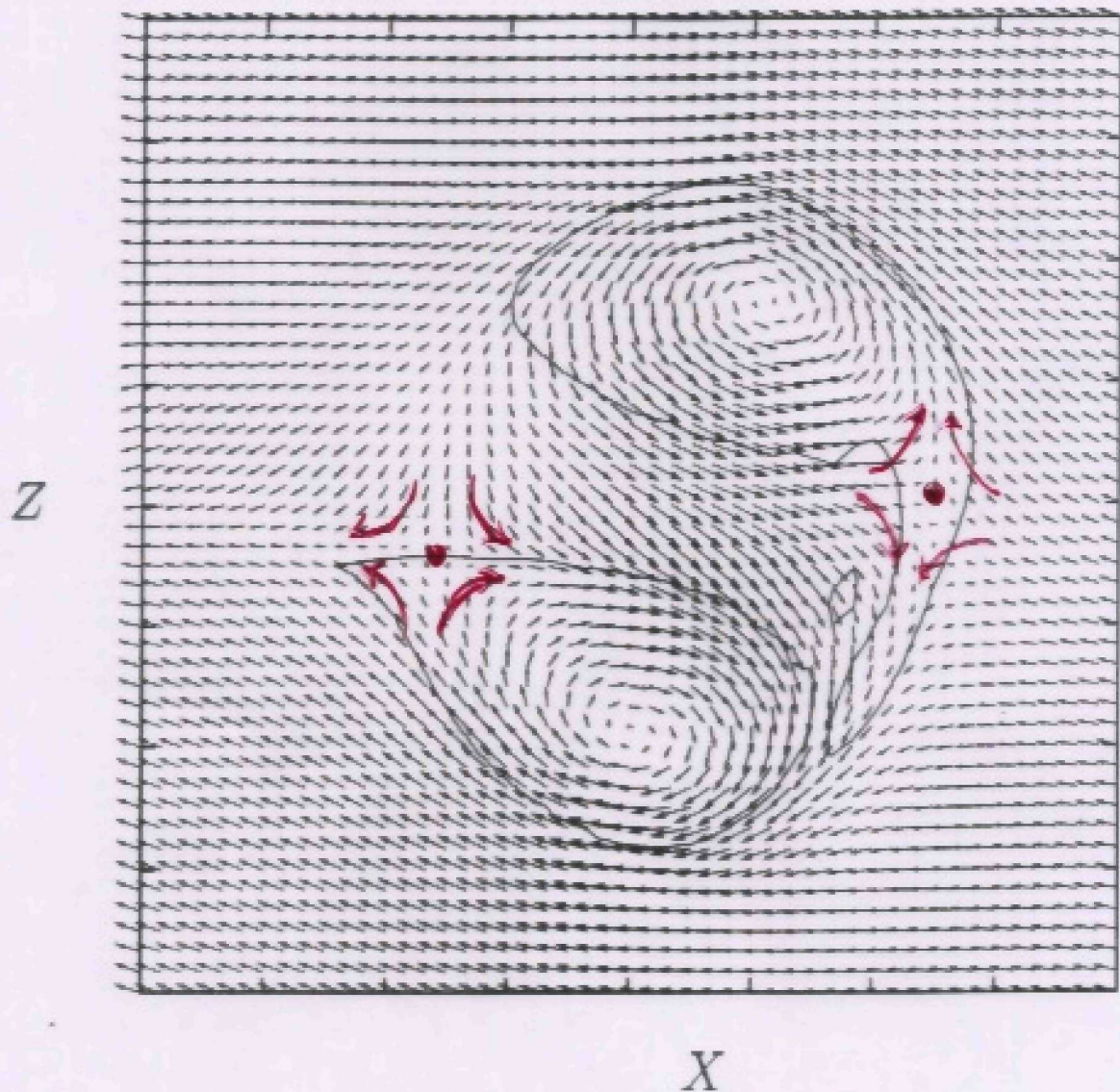


FIGURE 12: Contour plots of relative vorticity  $\omega_z$  in the horizontal symmetry plane  $z = 0$  of the water ring, obtained from a numerical simulation with  $Ro = 23$  and  $Re = 900$ : (a)  $t = 17$ , (b)  $t = 33$ , (c)  $t = 50$ , (d)  $t = 67$ , (e)  $t = 83$ , (f)  $t = 100$ , (g)  $t = 117$ , (h)  $t = 133$ , (i)  $t = 150$ . Contour increments  $\Delta\omega_z = \pm 0.1$ , minimum contour level at  $|\omega_z| = 0.1$ ; solid lines denote positive values and dashed lines negative values. The insets show the trajectories of the core centres, the instantaneous position of the vortex ring in each panel is denoted by black dots.



Velocity field  
(in a frame moving with the ring)

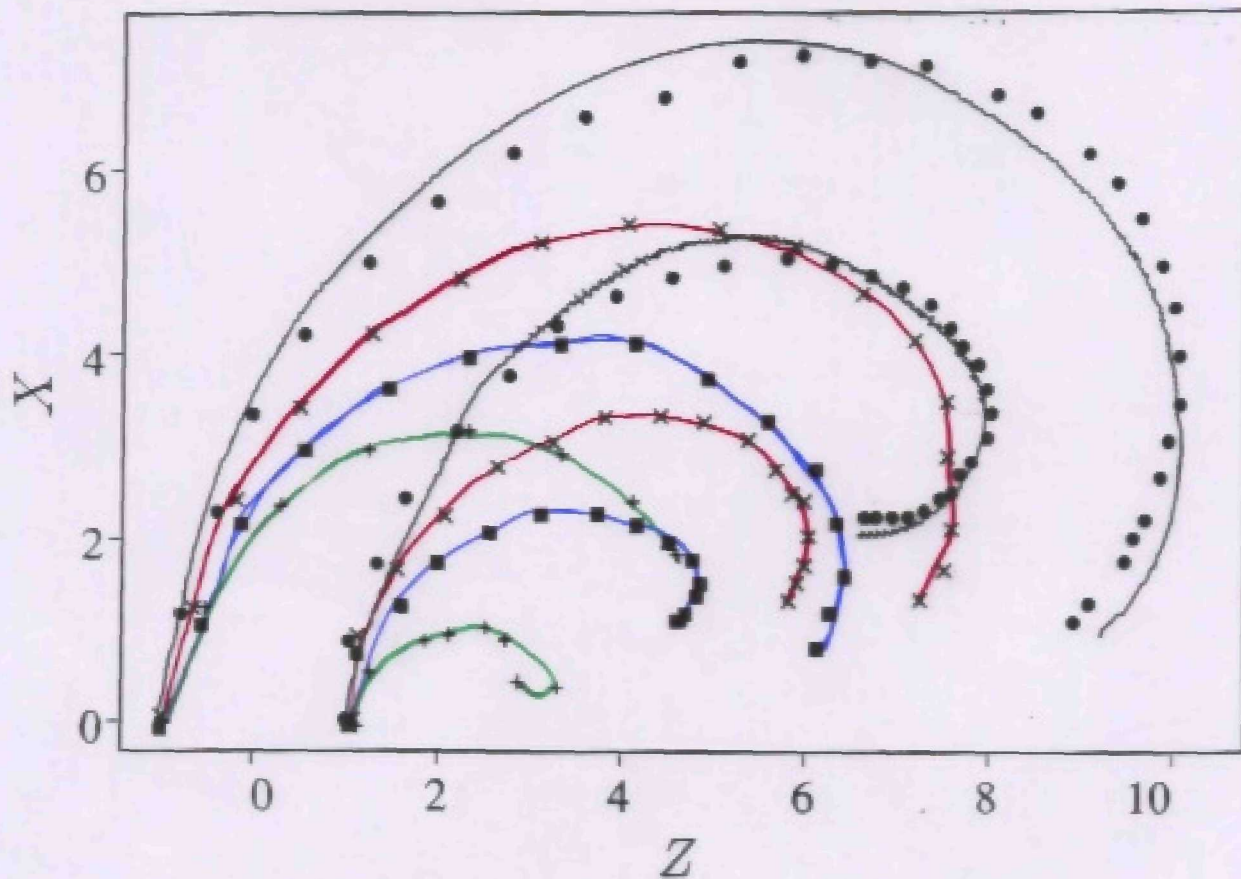


owing to the curved trajectory stagnation points are shifted inside the ring cores

vorticity filaments stripped from the vortex  $\implies$   
ring depletion

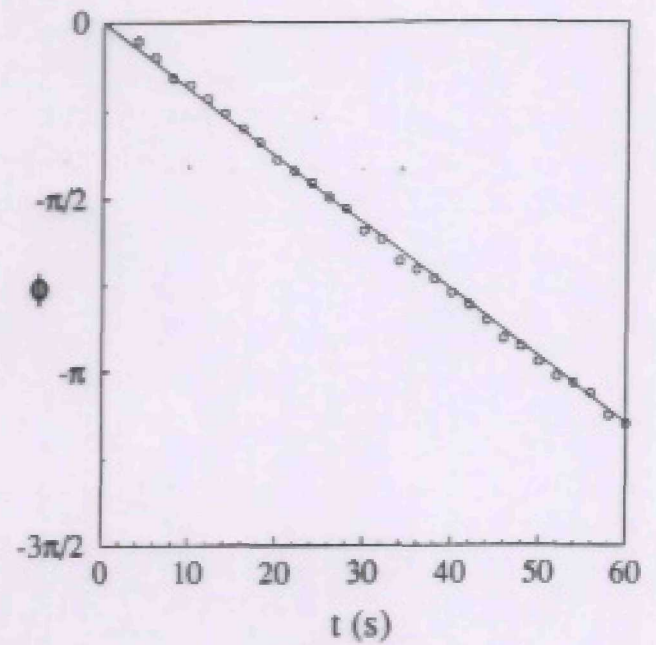
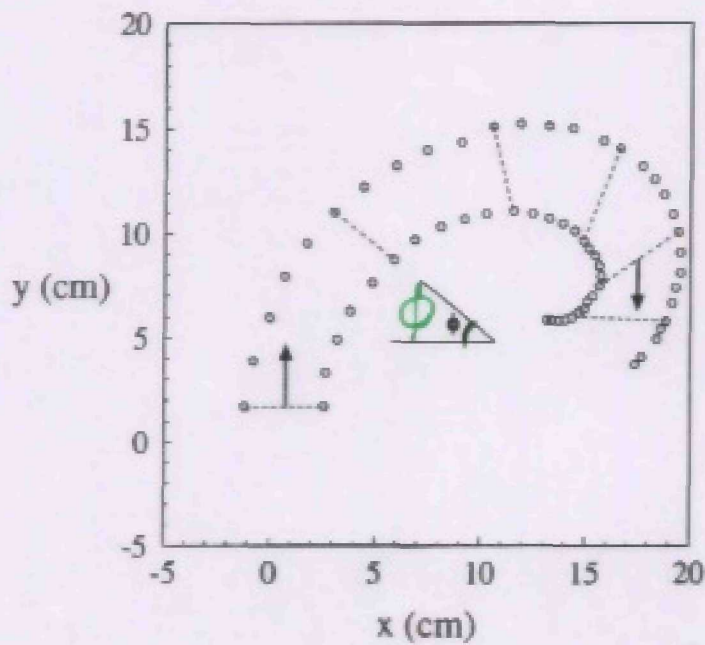
## Ring trajectories

- Curvature enhanced as  $Ro$  decreases



- $Ro = 23$ ,  $\times$   $Ro = 15.6$ ,  $\blacksquare$   $Ro = 12.7$ ,  $\blacktriangle$   $Ro = 8.2$ ,  
— numerical simulation at  $Ro = 23$ .

# Ring trajectory



$$\Omega_r = \frac{d\phi}{dt} = -\Omega$$

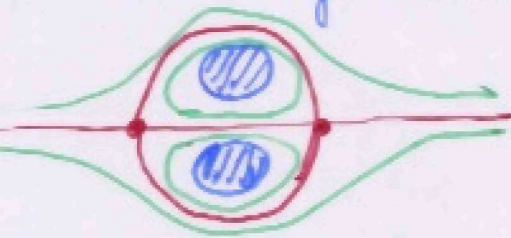
- straight path in an inertial frame

Exp.	$\Omega$ ( $s^{-1}$ )	$\Omega_r$ ( $s^{-1}$ )
1	0.06	$-0.06 \pm 0.002$
2	0.09	$-0.101 \pm 0.002$
3	0.11	$-0.12 \pm 0.002$
4	0.17	$-0.17 \pm 0.002$

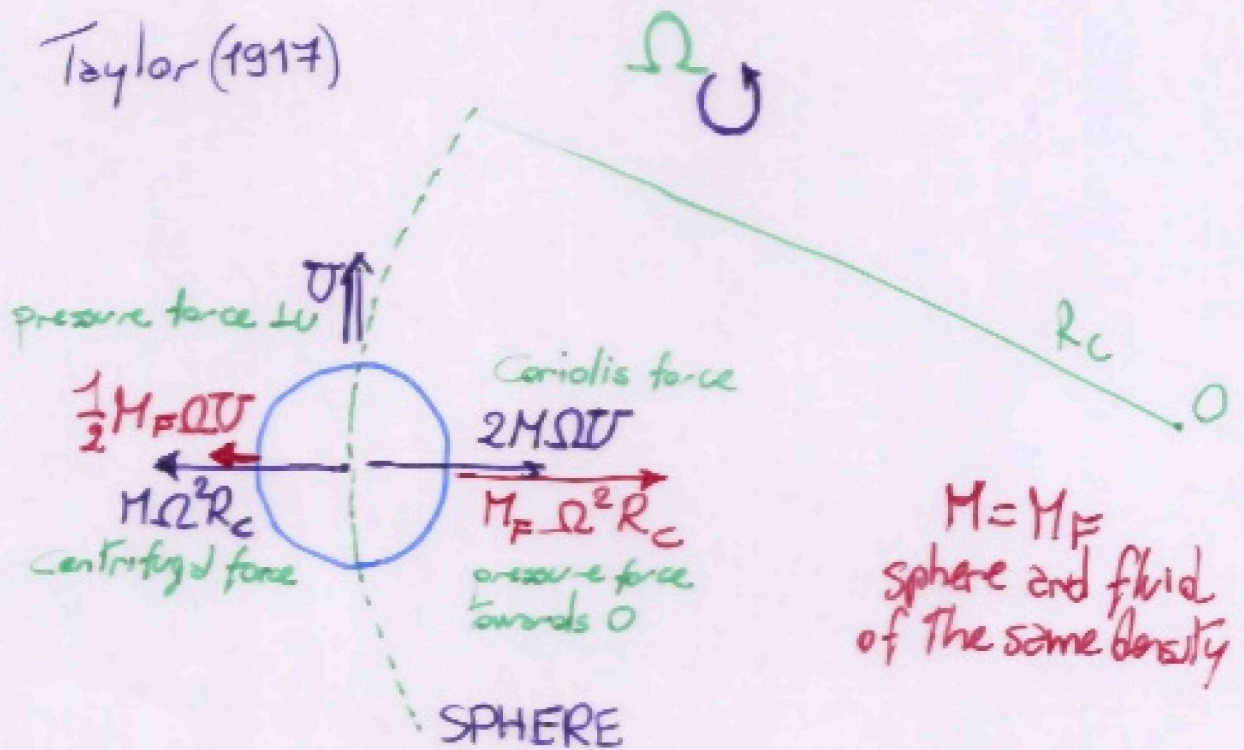
"Thick" rings carry a spherical blob of fluid

(not thin rings)

(Batchelor 1967)



From Taylor (1917)



$M = M_F$   
sphere and fluid  
of the same density

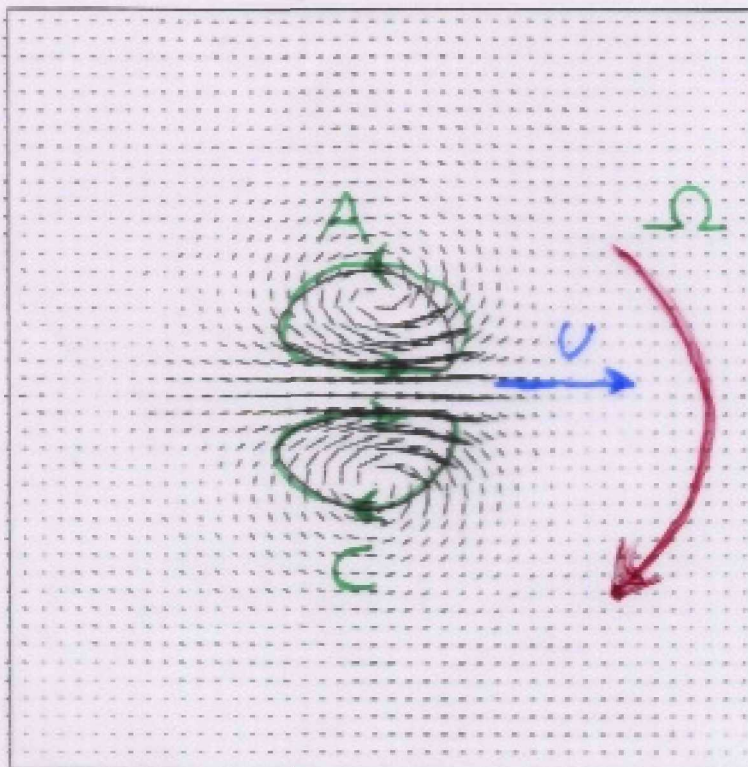
net force  $-\frac{3}{2} M \Omega U$  (Proudman 1946)  
(Taylor 1917)

sphere mass  $M + \frac{M}{2} = \frac{3}{2} M$  (Batchelor 1967)  
in a non rotating fluid  
added mass

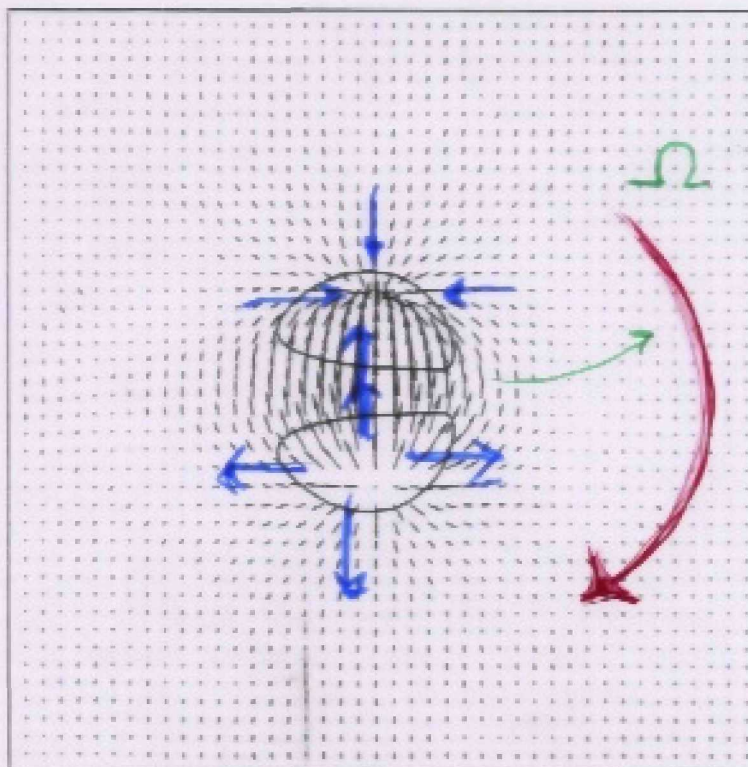
acceleration  $a_{\perp} = -\Omega U$   
centr. acc.  $a_c = U^2 / R_c$  }  $U = -\Omega R_c$

The sphere moves along a straight path  
in the inertial frame

anti-cyclonic side shrinks  
cyclonic side widens



Velocity

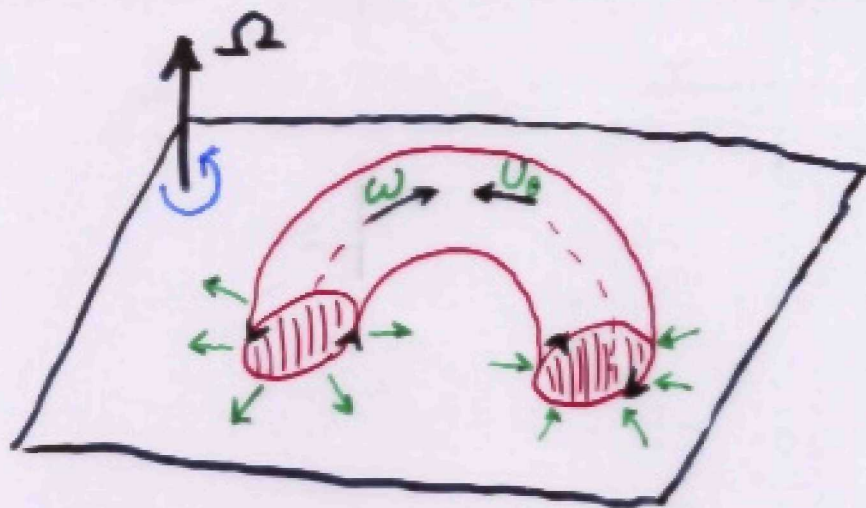


$$-2\Omega \wedge u$$

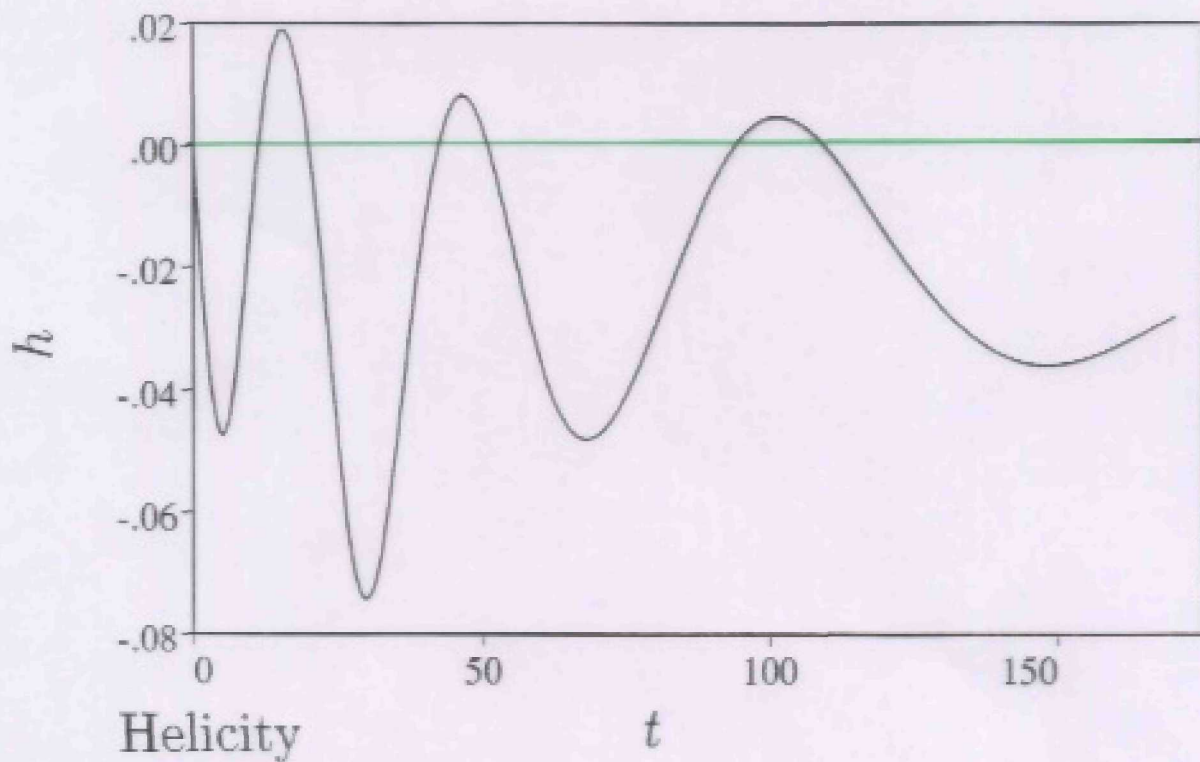
net force



Coriolis force

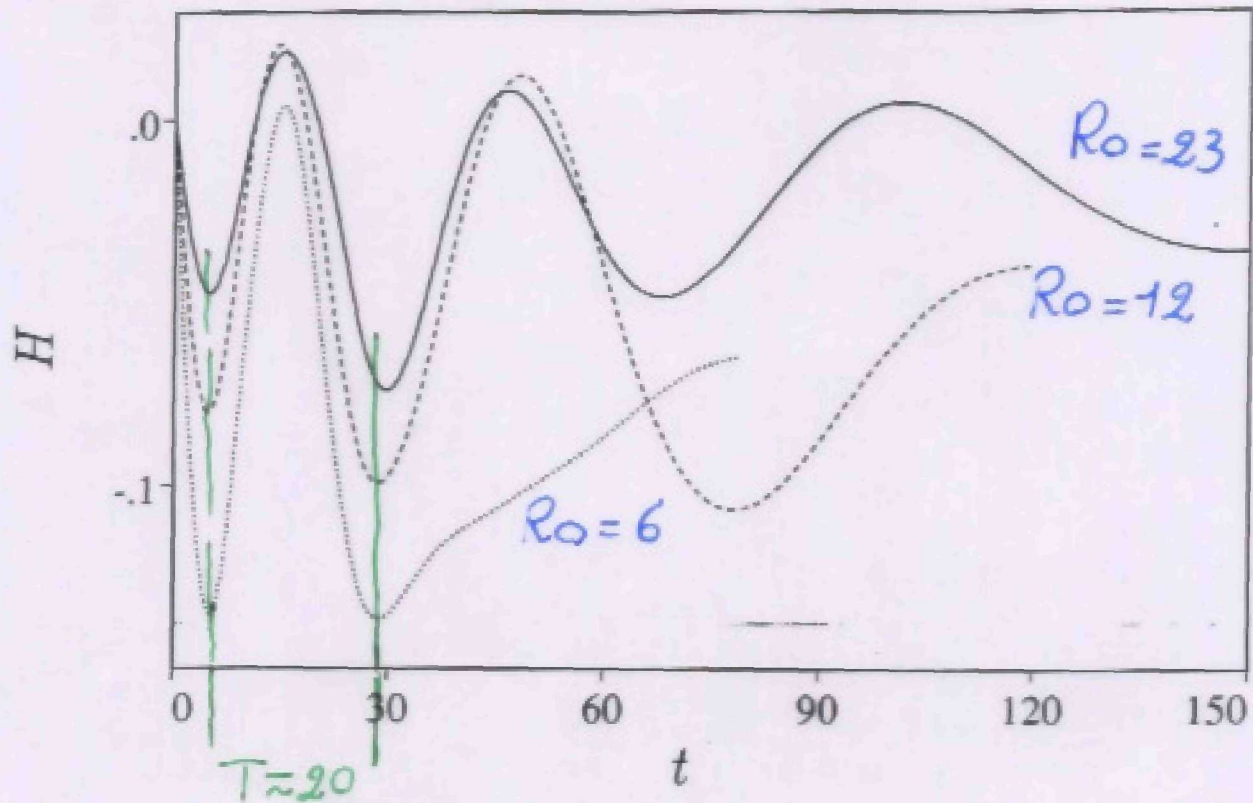


$$h = \int_V \omega \cdot \underline{u} dV < 0$$



vorticity differences can not be steadily maintained along a vortex tube  $\Rightarrow$   
Kelvin Waves

# Waves in the ring

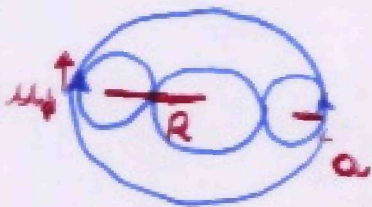


Oscillation period independent of  $Ro \implies$  Kelvin waves

oscillation period  $T = R/c$

$c$  celerity of the wave

$c \approx u_\phi$  (Kelvin 1880)

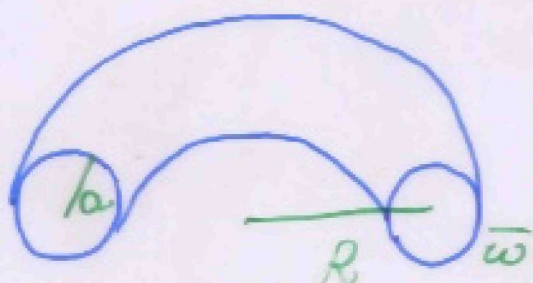


$$u_\phi \sim \frac{\Gamma}{a}$$

$$T \sim a R / \Gamma$$

non dimensional time

$$T_{\text{total}} = T \frac{\Gamma}{R^2} \sim a/R$$



from Saffman (1982)  $c \approx .417 \bar{w} a$   
from in. con.  $\bar{w} \approx 2$   $a \approx .4$



$$c \approx .33$$

Wave period

$$T = 2\pi R/c \approx 18$$

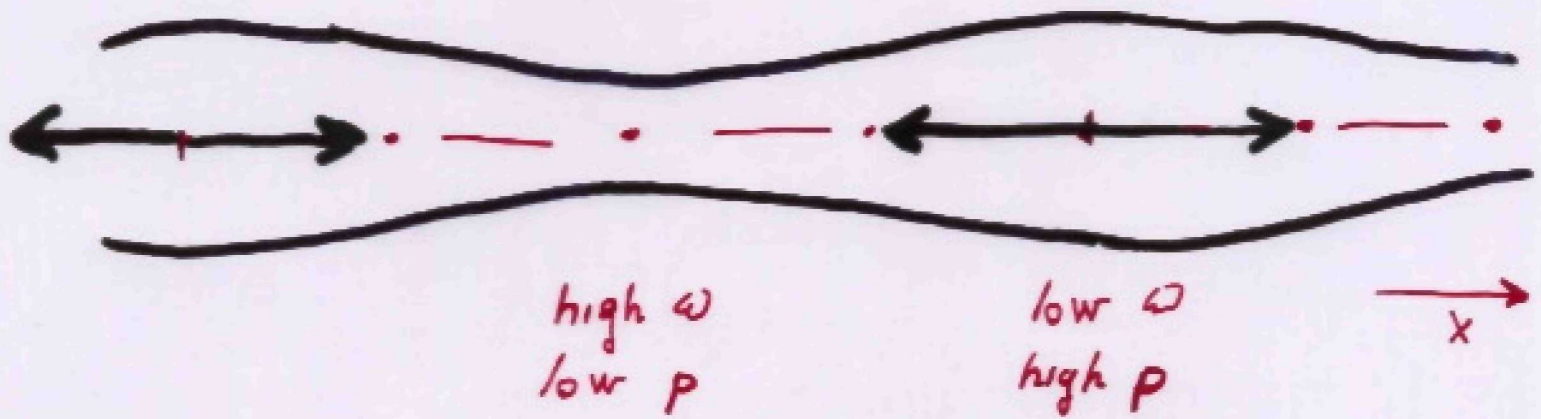


# Kelvin waves

Non uniform vortex with constant circulation  $\Gamma$

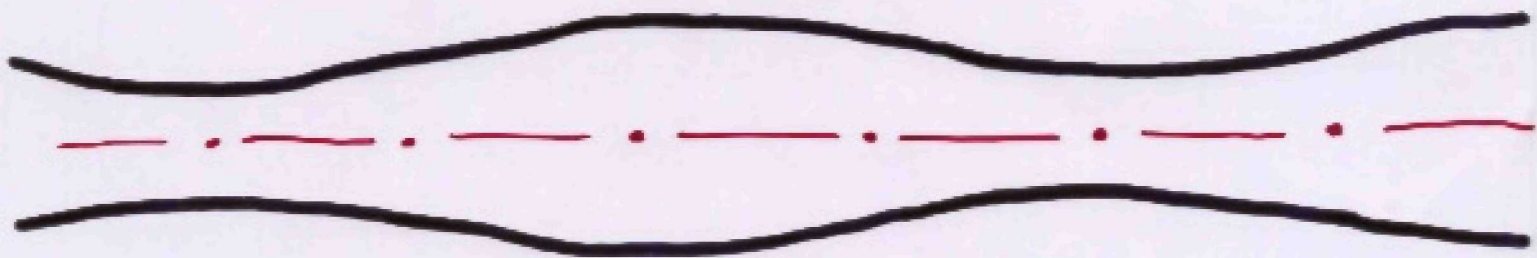
$$S_x < 0$$

$$S_x > 0$$



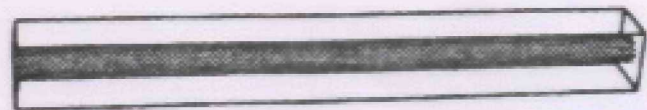
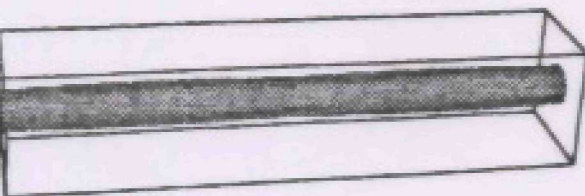
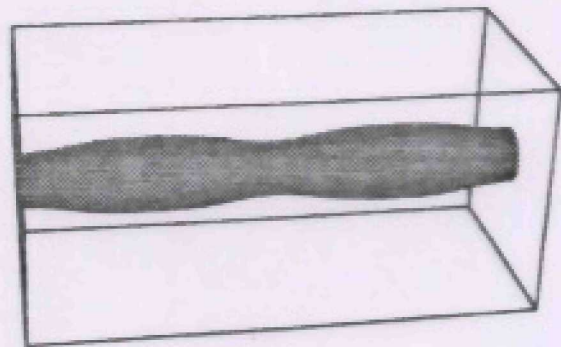
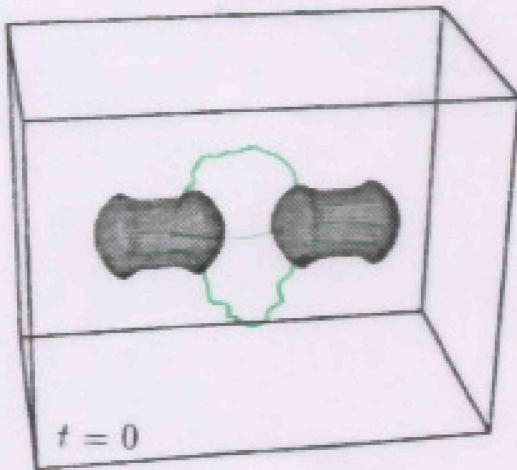
## • axial pressure gradient

- extensional strain in fat sections
- compressive strain in narrow sections



## Aligned strained sticks

- $Re_{\Gamma} = 200, Re_L/Re_{\Gamma} = 0.06$



$t = 16, L_x = 10.93, L_y = L_z = 2.42.$

$t = 24, L_x = 18.07, L_y = L_z = 1.88.$

- Burgers vortex  $\Rightarrow$  waves are compatible with stretching

- Uniform stretching  $\Rightarrow$  high velocities incompatible with turbulence statistics

# Wave mechanism works for structures not aligned

## Angled short vortices ('sticks')

- $Re_\Gamma = 200, S_0 = 0$ . (no strain)

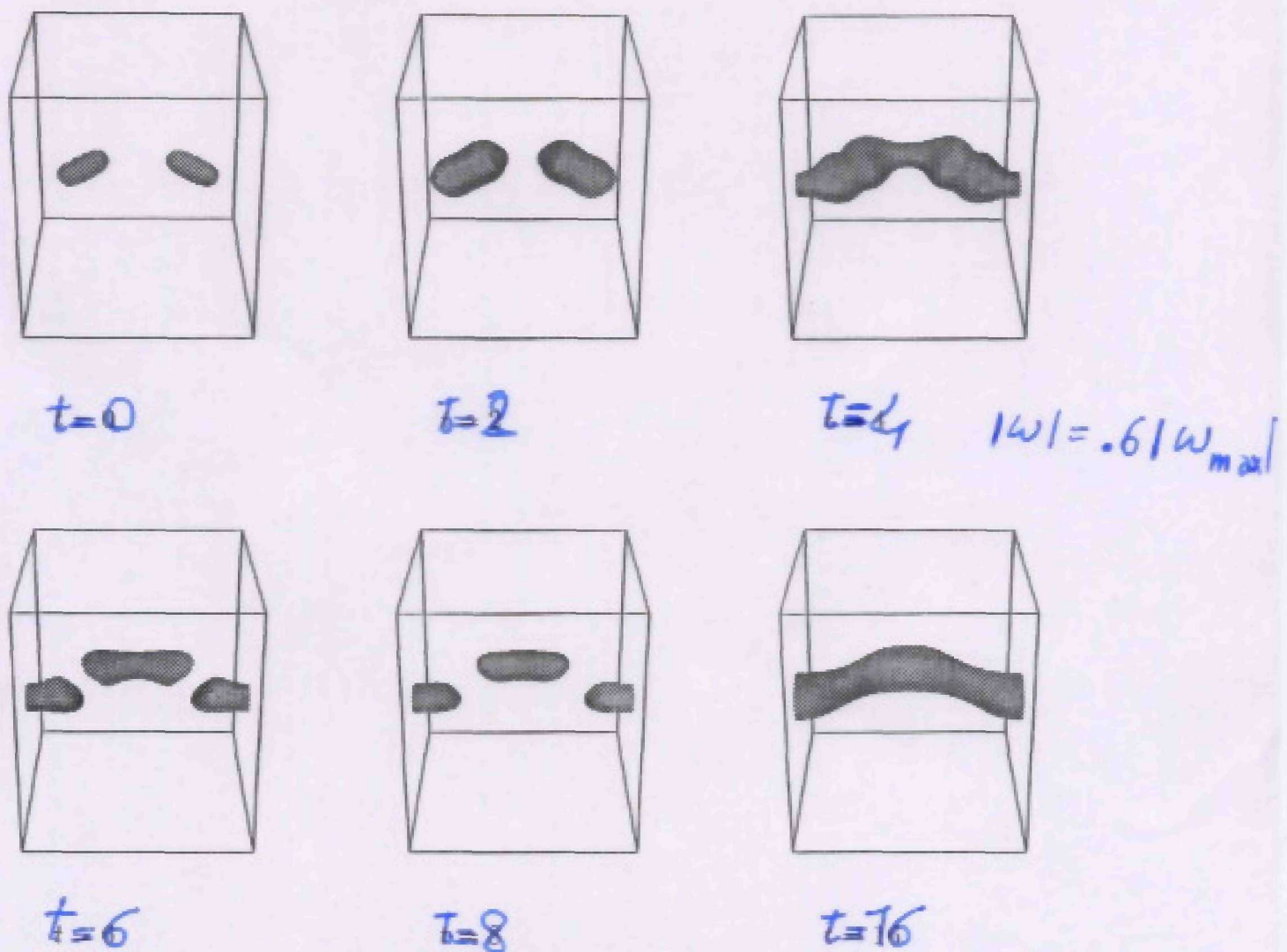


FIGURE 4. Iso-surfaces of vorticity magnitude for angled sticks at  $Re_\Gamma = 200$ . Iso-surface is always drawn at  $|\omega| = 0.6 |\omega_{max}(t)|$ . The initial angle between stick axes is  $120^\circ$ . ( $64 \times 64 \times 64$  grid).

- Uniform diffusing vortex

## Conclusions

(ring motion  $\parallel \underline{\Omega}$ )

- 'Low rotations': the ring slows down and weakens
- 'High rotations': formation of oblique shear layers
- 'Very high rotations': 2D Taylor column
- 3D: small misalignment very important.

## Related papers

Vortex rings { Verzicco et al. JFM, 317, 1996  
Eisenga et al. JFM 354, 1998

Vortex filaments { Verzicco Jimenez & Orlandi JFM, 299, 1995  
in "model"  
Tu-balance { Verzicco & Jimenez JFM, 394, 1999

## Conclusions

(Ring motion  $\perp \Omega$ )

- The ring follows a curved trajectory
- Straight path in an inertial frame
- The ring weakens in time owing to a peeling process
- The ring remains 'toroidal' up to the end of the evolution
- Future work: higher rotation rates